

Neutrino Emission by the Photo Production Process in a Hyper-Accretion Disk

David R. MacInnis

Submitted in partial fulfilment
of the requirements for the degree of
Master of Science

Saint Mary's University
Halifax, Nova Scotia

February, 2004

©2004 David R. MacInnis



National Library
of Canada

Bibliothèque nationale
du Canada

Acquisitions and
Bibliographic Services

Acquisisitons et
services bibliographiques

395 Wellington Street
Ottawa ON K1A 0N4
Canada

395, rue Wellington
Ottawa ON K1A 0N4
Canada

Your file *Votre référence*

ISBN: 0-612-92052-6

Our file *Notre référence*

ISBN: 0-612-92052-6

The author has granted a non-exclusive licence allowing the National Library of Canada to reproduce, loan, distribute or sell copies of this thesis in microform, paper or electronic formats.

L'auteur a accordé une licence non exclusive permettant à la Bibliothèque nationale du Canada de reproduire, prêter, distribuer ou vendre des copies de cette thèse sous la forme de microfiche/film, de reproduction sur papier ou sur format électronique.

The author retains ownership of the copyright in this thesis. Neither the thesis nor substantial extracts from it may be printed or otherwise reproduced without the author's permission.

L'auteur conserve la propriété du droit d'auteur qui protège cette thèse. Ni la thèse ni des extraits substantiels de celle-ci ne doivent être imprimés ou autrement reproduits sans son autorisation.

In compliance with the Canadian Privacy Act some supporting forms may have been removed from this dissertation.

Conformément à la loi canadienne sur la protection de la vie privée, quelques formulaires secondaires ont été enlevés de ce manuscrit.

While these forms may be included in the document page count, their removal does not represent any loss of content from the dissertation.

Bien que ces formulaires aient inclus dans la pagination, il n'y aura aucun contenu manquant.

Canada

Table of Contents

List of tables.....	iv
Examining Committee.....	v
Acknowledgements.....	vi
Abstract.....	vii
Chapter 1 - Introduction	1
1.1 Supernova Explosions.....	1
1.2 Outline.....	4
Chapter 2 - Hypernovae & Hyper-Accreting Black Holes	6
2.1 Hypernovae or “Failed” Supernovae.....	6
2.2 Evidence of Hypernovae.....	8
2.3 White Dwarf and Black Hole Merger.....	9
2.4 Helium Star and Black Hole Merger.....	10
2.5 Neutron Star and Black Hole Merger.....	11
2.6 Hyper-accreting Black Holes.....	11
2.7 Hypernova Models.....	13
2.8 Neutrino Emission from Models.....	14
2.9 Neutrino Cooled Accretion Disks.....	15
Chapter 3 - Neutrino Emissivity & Rates	18
3.1 Neutrino Production in Jets.....	18
3.2 Neutrino Production in Accretion Disks.....	20
3.2.1 Pair Neutrino Emission.....	20
3.2.2 Plasma Neutrino Emission.....	21
3.2.3 Recombination Neutrino Emission.....	22
3.2.4 Bremsstrahlung Neutrino Emission.....	23
3.2.5 Photo Neutrino Emission.....	24
3.3 Neutrino Detection.....	26
3.4 Summary.....	27
Chapter 4 - Results & Conclusions	29
4.1 Monté Carlo Method.....	29
4.2 Results.....	30
4.3 Conclusions.....	33

Chapter 5 - Supernova 1987A	36
5.1 Neutrino Detection.....	36
5.2 Discussion.....	38
Appendix A - Code for Determining the Electron Chemical Potential	41
Appendix B - Code for the Photo Neutrino Emissivity & Rates	47
References.....	75
Curriculum Vitae.....	78

List of Tables

Table 1	Summary of parameters of likely hyper-accreting disks.....	12
Table 2	Hypernova Model parameters	17
Table 3	Emissivity and rate of neutrinos from different processes.....	28
Table 4	Comparison of the results	34

Acknowledgements

First of all, I would like to thank Saint Mary's University and the Department of Astronomy and Physics for giving me the privilege to attend and study here at Saint Mary's. Between the years of 2000 and 2002, the department and the university have funded me in the forms of scholarships and jobs like research and lab assistants. Without this financial help, my stay at Saint Mary's could not have happened.

All of this work could not have materialized without the guidance of Dr. Malcolm Butler. He was there with me throughout the whole process, helping and pushing me along the way. His insight and aid were invaluable to me. During some stretches I was in his office every day, sometime just five minutes sometimes an hour and I want to thank him for all the time he has put into this thesis.

I would also like to thank my committee that consisted of Dr. Malcolm Butler, Dr. Gary Welsh, Dr. Ian Short, and the external reader Dr. Rachid Ouyed. They took the time to read my thesis and give me insights to where my thesis should be headed. Their help was very constructive it is a better piece of work for it.

I would also like to thank the other members of the faculty. Dr. David Guenther, Dr. Gary Welsh, and Dr. Phil Bennett has spent many hours with me and the other graduates in the classroom. I've appreciated the time you have spent teaching us the many wonders that exist in our universe. Dr. David Turner and I had many fun hours spent in the lab. Dr. Mitchell, Dr. Adam Sarty, Dr. David Clarke, Dr. Nick Tohill, and Dr. Francine Marleau, we've had heated debates during Journal Club. David Lane had solved any computer problems I had thrown at him and Elfrie Waters had answered many questions that I have had during this two year process.

Much of my time at Saint Mary's was spent in the grad room. Over my two years I had the privilege to spend that time with Peter, Andrew, Kevin, Louise, and Glenn. We've spent many hours discussing papers, assignments, labs, the students in the labs, and where we are going to spend our Thursday and Saturday nights.

Finally, I would like to thank my family, Mom, Dad and my brother Mike. They have been behind me 100% since the day I set foot on this Earth. With lots of love and the occasional check in the mail (if you ask them they'll tell you they were more frequent) they have supported me the whole way. I love you all and I want to dedicate this thesis to my family.

Neutrino Emission by the Photo Production Process in a Hyper-Accretion Disk

Abstract

MacFadyen & Woosley (1999) have studied two models of a hypernova, where a hyper-accreting disk is created in the core of a star. Their code requires an accurate model of local energy loss given by neutrino emission. An emissivity of 3.5×10^{34} ergs cm^{-3} s^{-1} can be calculated using conservation laws of an accretion disk around a black hole.

MacFadyen & Woosley (1999) used 9×10^{34} ergs cm^{-3} s^{-1} in their models. In particular, in this thesis, I analyze the contribution of the photo neutrino process to the emissivity. For a temperature of 10^{10} K, a density of 10^9 g/cm^3 , and a chemical potential of 2.02×10^7 eV, emissivities of $(8.7 \pm 0.1) \times 10^{21}$ and $(7.0 \pm 0.2) \times 10^{21}$ ergs cm^{-3} sec^{-1} are found. Rates of $(8.6 \pm 0.1) \times 10^{26}$ and $(7.3 \pm 0.2) \times 10^{26}$ cm^{-3} sec^{-1} are also found with average neutrinos energies of (6.2 ± 0.2) and (6.0 ± 0.3) MeV. The calculation of the photo neutrino production process is a more robust calculation than seen in previous work with the use of the complete scattering amplitude, and the use of Monte Carlo integration methods.

David R. MacInnis

February, 2004

Chapter 1

Introduction

1.1 Supernova Explosions

The exact mechanism that causes stars to end their lives as a supernova is unknown. Models suggest that low-mass stars experience their deaths via a planetary nebula, where temperatures inside the core cannot increase sufficiently to continue the chain of reactions required to produce iron. A white dwarf or the core is left intact, composed mostly of carbon.

For stars with larger mass, the core is able to generate higher temperatures due to the greater gravitational potential. The core, after tens of millions of years, is able to begin producing iron. When iron is produced in the core, no more energy or photons can

be produced through fusion because iron is the most stable of all the elements. At this point, the star is not in hydrodynamic equilibrium because the force of gravity is not in equilibrium with the radiation pressure from photons produced in the core. Therefore gravity causes the star to start to collapse in on itself. A shock is formed and travels through the star, bouncing off of the core or proto-neutron star causing it to form into a neutron star. After the shock bounces off of the core it travels through the star causing it to blow up in a spherically symmetric explosion known as a supernova.

For even more massive stars, the core bounce mechanism is also invoked for the cause of the explosion of these stars. Modeling of such explosions sees that the shock, after the bounce off of the core, seems to stall in the thicker mantles of oxygen and silicon (Kifonidis et al. 2003). The models use deep convection into the core to re-energize the stalled shock. The convection dredges up neutrinos, electrons, and positrons and deposits these energetic particles right under the stalled shock. After the shock is re-energized, it travels through the rest of the star and again blows up the star in a spherically symmetric explosion.

This convection is added to the models because the core bounce mechanism alone is unable to produce a supernova, and we know that these stars do indeed explode (Kifonidis et al. 2003). Whether this convection actually occurs is unknown at this time but it does explain how these stars could experience a supernova. One way of testing if this model is correct is by studying the difference in neutrino fluxes from these two models, with or without convection.

Extremely massive stars (larger than 25 to 35 solar masses) contain denser, thicker mantles of oxygen and silicon overlying the collapsing iron core (MacFadyen & Woosley 1999). The mechanism of core bounce with convection breaks down and models of these stars do not produce supernovae (MacFadyen & Woosley 1999). We know that these stars do experience supernova explosions, so another mechanism or additional contributions to the core bounce model are needed.

MacFadyen & Woosley (1999) follow, in models, the evolution of these shocks. They confirm that, even with convection into the core, this mechanism cannot explode the star. The shock stalls and can never be re-energized. In those cases the standard mechanism may “fail” to produce a supernova because the proto-neutron star will accrete matter before an explosion develops, causing it to collapse to a black hole. For these models the term “failed supernova” has been used to describe them.

MacFadyen & Woosley (1999) decided to study the accretion onto the proto-neutron star instead of focusing on the shock. They found that the proto-neutron star accreted enough matter, before the shock exploded the star, to cause its collapse into a black hole. An accretion disk forms around the black hole and jets are then formed above and below the poles of the black hole. The jets then blow up the star in an axially symmetric explosion. The term given to this mechanism is a hypernova explosion.

1.2 Outline

Evidence for hypernovae is discussed in Chapter 2 along with the models that MacFadyen & Woosley (1999) have analyzed. Other hyper-accreting disks that could also produce similar temperature and density environments are compared to those of the hypernova model. In particular the energy loss rate through neutrinos is discussed. Descriptions of neutrino-cooled accretion disks are considered to provide an estimate of their neutrino emission rates.

Neutrino emissivity and rates are discussed in Chapter 3 along with means for their possible detection. In particular, high energy neutrinos will be produced in jets associated with the hyper-accreting disk, along with low-energy quasi-thermal neutrinos produced within the disk. The specific production processes of these thermal neutrinos will be discussed, such as the pair and plasma production processes. The photo production process is discussed in more detail with the complete scattering amplitude.

The photo neutrino emission process, a dominant mechanism for neutrino production in an environment like the accretion disk produced by a hypernova, is calculated in Chapter 4 using the Monte Carlo method. Results for the photo neutrino emissivity, rates, and average neutrino energy from the accretion disk of one of MacFadyen & Woosley's (1999) hypernova models are reviewed in Chapter 4. The potential for Super-Kamiokande to detect these neutrinos is also discussed.

In Chapter 5, the neutrinos detected from supernova 1987A are discussed, along with how they could be related to the neutrinos produced from a hyper-accreting disk. I will discuss a possible connection between SN 1987A and hypernovae.

Chapter 2

Hypernovae & Hyper-accreting Black Holes

2.1 Hypernovae or “Failed” Supernovae

MacFadyen & Woosley (1999) present a model that is based on the supposition that larger stars may experience a supernova that is different from the expected mechanism of a neutrino heated shock. The exact mechanism whereby the collapsing iron core of a massive star produces an outgoing shock and creates a supernova remains uncertain. As mentioned earlier, modern calculations suggest that the explosion is powered by neutrino energy deposition in a hot, convectively unstable, bubble of radiation and electron-positron pairs just outside the proto-neutron star. The deposition of energy re-ignites the stalled shock which then propagates through the star's envelope.

In the model of the hypernova, if the star has no angular momentum, the star will fall onto the black hole in a hydrodynamical timescale and simply disappear. In the realistic situation, where the star is spinning, then the mantle and outer layers of the star will fall freely inside the last stable orbit around the black hole, $r_{\text{iso}} = 2.7 \times 10^6 (M_{\text{BH}} / 3 M_{\odot})$ cm, creating an accretion disk (McFadden & Woosley 1999). The accretion rate onto the black hole is on the order of 0.1 solar masses per second (McFadyen & Woosley 1999).

Large energy deposition can occur in the polar regions of the black hole through neutrino annihilation and magnetohydrodynamical processes, but jet production cannot commence until the density in the polar regions has declined to 10^6 g/cm³ (MacFadyen & Woosley 1999). Jet formation may be delayed until most of the accretion and energy generation is over, at which point the jets blow aside what remains of the star within about 10 to 20 degrees of the poles. This will blow the star up in an axially driven “supernova.”

The formation of a massive, rapidly rotating star is probably favored by low metallicity. The low metallicity keeps the radius of the star smaller, increases angular momentum, and reduces mass loss (MacFadyen & Woosley 1999). A close binary star may be needed to help remove the envelope to expose the bare helium core (Wolf-Rayet star), and to help increase the angular momentum inside the core to enable higher accretion rates. This will lead to higher temperatures and more energetic neutrinos, in turn depositing more energy above and below the poles of the black hole.

2.2 Evidence of Hypernovae

Wang (1999) has looked at previously classified supernova remnants and has calculated inferred blast-wave energies of around 3×10^{52} ergs for NGC 5471B and around 3×10^{53} ergs for MF 83. He suggests that these remnants likely originated as hypernovae, since the energies involved here are too large for the typical supernova mechanism to produce.

Evidence of hypernovae can also be seen in signatures of gamma-ray bursts. MacFadyen & Woosley (1999) postulated X-ray precursors to the gamma-ray bursts, which are created when the jets first break out of the star. Fargion (2001) has found that gamma-ray bursts GRB 971210, 971212, 990518, 000131 all have been observed to emit these X-ray precursors.

Radiation from cobalt, nickel, and iron is also expected to be emitted by the inner engine for a couple of days after the bursts (McLaughlin et al. 2001). From the optical afterglow of the gamma-ray burst GRB 980425, detected by the Beppo-SAX satellite, Fynbo et al. (2000) state that the burst is located in the galaxy ESO 184-G82. Fynbo et al. (2000) claim to have detected the signatures of the elements magnesium, silicon, sulphur, argon, and calcium - material most likely found in an expanding debris cloud produced by the explosion of a massive star. Fynbo et al. (2000) believe that is evidence that the gamma-ray burst is linked to a very energetic "supernova" explosion which may have preceded the powerful flash of gamma-rays.

Lazzati et al. (2001) have presented photometric and spectroscopic observations of the late afterglow of GRB 000911, where the R, I, and J light-curves were observed to have a significant re-brightening which can be explained by the presence of an underlying “supernova.”

Another class of models with the same accretion disk environment arise from mergers of stellar objects with black holes. Possible stellar objects are white dwarf, helium, and neutron stars. A short discussion of these accretion disks, and how their temperature and densities will differ from that of a hypernova, will follow.

2.3 White Dwarf & Black Hole Merger

The merger of a stellar object with a black hole, the tidally-disrupted object forms an accretion disk around the black hole that should have the same environment as a hypernova. The merger of a white dwarf and a black hole has also been proposed by Fryer et al. (1999) to explain long-duration gamma-ray bursts. In order to determine the energy to power ratio, one must determine the accretion rate and the angular momentum of these disks, which in turn depend upon the size and mass of the accretion disk (Fryer et al. 1999). Therefore, it is important to determine how quickly and at what radius the white dwarf is torn up by the gravitational potential of the black hole and transformed into an accretion disk.

To accurately calculate the mass transfer and mass accretion rate onto the black hole, Fryer et al. (1999) used a three-dimensional hydrodynamical small particle code (Davies et al. 1991). Their simulations showed that after losing around 0.2 solar masses, the mass transfer rate becomes so large that the white dwarf becomes disrupted and, within roughly an orbit time, what remains of it becomes part of the accretion disk around the black hole. Peak accretion rates are ~ 0.05 solar masses per second (less for lower mass white dwarfs) and last for approximately a minute.

The accretion disk will cool via neutrino emission, which is then converted into electron - positron pairs via neutrino annihilation. The energy released, with beaming factor on the order of 100 in an optimistic situation, could be on the order of 10^{47} ergs to 5×10^{50} ergs (Fryer et al. 1999). The possibility of a strong magnetic field produced in the accretion disk, which can tap into the rotational energy of the black hole, could help add power to the production of jets on the order of 10^{48} ergs to 4×10^{49} ergs.

2.4 Helium Star & Black Hole Merger

Fryer and Woosley (1998) propose a model that tries to explain the longer duration bursts, in which a stellar-mass black hole acquires a massive accretion disk by merging with the helium core of its red giant companion. Like the white dwarf and black hole merger model, the energetics of this model depends on the accretion rates onto the black hole. Fryer & Woosley (1998) estimate that the maximum energy from

electron-positron pairs is around 10^{48} to 10^{52} ergs.

2.5 Neutron Star & Black Hole Merger

Janka et al. (1999) state that, unlike the merger of a white dwarf or helium star with a black hole, the material accretes onto the black hole more rapidly due to the compactness of the material inside the neutron star. This will cause temperatures and densities in the accretion disk to be different than the models discussed above.

Janka et al. (1999) set up hydrodynamic simulations of this merger with Newtonian calculations, and they find that the mechanics of the neutron star's destruction depend greatly on the ratio of mass between the two objects. During the first inspiral, the mass transfer to the black hole can have rates up to 1000 solar masses per second. Within 2 to 3 milliseconds the neutron star can lose 50% to 75% of its initial mass. What is left is an accretion disk around the black hole with mass around 0.3 to 0.7 solar masses. In a matter of 10 to 20 milliseconds an energy of $\leq 10^{51}$ ergs will have been deposited above the poles of the black hole where a mass of 10^5 solar masses may lie.

2.6 Hyper-accreting Black Holes

The major difference between each of the models of interest is the accretion rate

onto the disk and eventually onto the black hole. The varying accretion rate, disk and black hole masses produces different environments, in terms of temperature and pressure scales, around the black hole. This produces a varying neutrino emission for each model. The various parameters of the models are listed in Table 1.

Models of Interest	Duration (seconds)	Available Energy (ergs)	Neutrino Luminosity (ergs per second)	Accretion Rates (solar masses per second)
NS / BH	0.1	$10^{50} - 10^{51}$	$10^{51} - 10^{52}$	10 - 1000
WD / BH	15 - 150	$10^{46} - 10^{50}$	$10^{43} - 10^{49}$	0.01 - 0.07
He / BH	15 - 500	$10^{46} - 10^{51}$	$10^{43} - 10^{50}$	1
Hypernova	5 - 20	$10^{50} - 10^{53}$	$10^{49} - 10^{52}$	0.1 - 1

Table 1: Summary of parameters of likely hyper-accreting disks.

A viable mechanism to release energy, on the order of 10^{46} to 10^{53} ergs from the accretion disk is neutrino transport (Woosley 1993). The energy dissipated during accretion will be approximately $Mc^2/12$ (Shakura & Sunyaev 1973) where M is the mass accreted onto the black hole. The majority of emitted neutrinos will come from the last stable orbit around the black hole, which has a radius of 30 to 100 km. The neutrino emission of 10^{50} ergs per second should be converted into electron - positron pairs which will have a luminosity of (Ruffert et al. 1997):

$$L_{\text{pair}} \approx 3 \times 10^{46} \left(\frac{L_{\nu}}{10^{51} \text{ ergs s}^{-1}} \right)^2 \left(\frac{\langle \varepsilon_{\nu} \rangle}{13 \text{ MeV}} \right) \left(\frac{20 \text{ Km}}{R_d} \right) \text{ ergs s}^{-1} \quad (1)$$

where L_{ν} is the total neutrino luminosity of all flavors, $\langle \varepsilon_{\nu} \rangle$ is the mean neutrino energy,

and R_d is the inner disk radius. In the case where baryon contamination is high, neutrino-electron scattering may play a role in depositing an additional 10^{50} ergs per second in the regions of interest (Woosley 1993).

2.7 Hypernova Models

MacFadyen & Woosley (1999) used a two-dimensional hydrodynamic code to explore the continued evolution of a rotating helium star with masses greater than ten solar masses. In one model, the total energy deposited along the rotational axes by neutrino annihilation is $1-14 \times 10^{51}$ ergs, and the jets penetrated the star in about ten seconds.

Using their two-dimensional hydrodynamics code, MacFadyen & Woosley (1999) produced two models for hypernovae with different masses. Their first model evolved a 9.15 solar mass helium core from a 25 solar mass precursor. This helium star had a 1.78 solar mass iron core and had a radius of 2300 km. A second model was generated with a 14.13 solar mass helium star from a 35 solar mass star. The iron core in the second model had a mass of 2.03 solar masses.

These models were followed for roughly 20 seconds during three stages of evolution. The first stage is a transient stage lasting 2 seconds where matter above and below the poles falls freely onto the black hole while a centrifugally supported disk

forms in the last stable orbit around the black hole. During the second stage, which lasts 15 seconds, material falls onto the black hole from the accretion disk at the same rate at which material is falling onto the outer edge of the disk. For the 14 solar mass helium star model, this accretion rate is approximately 0.07 solar masses per second. The third stage is the explosion of the star, which occurs on a longer timescale than the 3 remaining seconds monitored in the models. Energy is deposited near the poles of the black hole and jets form, blowing away what remains of the star.

2.8 Neutrino Emission from Models

In the accretion disk created by a hypernova, temperatures can reach up to 10^{11} K at $r \sim 10^6$ cm and 10^9 K at $r \sim 10^9$ cm while densities can reach 10^{10} g cm $^{-3}$ (MacFadyen & Woosley 1999). At these temperatures, atoms are photodisintegrated into free neutrons, protons, and electrons. Neutrinos are the dominant source of cooling, as the disk is optically thin to them. MacFadyen & Woosley (1999) treat the emission as a local energy loss and use an approximation of neutrino emission from pair capture taken from Itoh et al. (1990):

$$\mathcal{E}_{\text{pair-cap}} = 9 \times 10^{33} T_{11}^6 \rho_{10} X_{\text{nuc}} \text{ ergs cm}^{-3} \text{ s}^{-1} \quad (2)$$

where $T_{11} = T/10^{11}$ K, $\rho_{10} = \rho/10^{10}$ g cm $^{-3}$, and X_{nuc} is the free nucleon mass fraction.

2.9 Neutrino Cooled Accretion Disks

To estimate and understand the emissivity of neutrinos from an accretion disk, one must understand the evolution of the disk. This in turn depends on the accretion rate, disk viscosity, and black hole mass. The mass of the disk varies roughly inversely with the viscosity parameter (MacFadyen & Woosley 1999). There are also a number of conservation laws that must be obeyed.

1) The conservation of mass equation is (Gammie & Popham 1998):

$$\dot{M} = 4\pi r h \rho V_r \quad (3)$$

where \dot{M} is the accretion rate, r is the radius, h is the height of the disk, ρ is the rest mass density, and V_r is the radial velocity of the disk and is measured in a co-rotating frame.

2) The equation of angular momentum conservation is (Gammie & Popham 1998):

$$\dot{M}(GMr)^{1/2} = 4\pi r^2 h \alpha P \quad (4)$$

where G is the Newtonian gravitational constant, M is the mass of the black hole, α is the viscosity parameter, and P defines the pressure.

3) The gas energy equation is (Gammie & Popham 1998):

$$\rho V_r \left(\frac{\partial U}{\partial r} \right) + P \left(\frac{\partial V_r}{\partial r} \right) + \frac{P V_r}{r} = \Phi - \varepsilon \quad (5)$$

where U is the internal energy parameter and (Mahadevan & Quataert 1997):

$$\left(\frac{\partial U}{\partial r}\right) = \left(\frac{P}{\rho^2}\right) \times \left(\frac{\partial \rho}{\partial r}\right) \quad (6)$$

The dissipation function, ε , is dominated by neutrino emission at these high temperatures, and Φ is the viscous heating rate which is equal to (Becker et al. 2001):

$$\Phi = \rho \alpha c_s \text{hr} \left(\frac{\partial \Omega}{\partial r}\right)^2 \quad (7)$$

where c_s is the local sound speed and $d\Omega/dr$ is the differential rotation of the disk and equals (Narayan et al. 1997):

$$\frac{\partial \Omega}{\partial r} = \frac{V_r \Omega_k (\Omega r^2 - j)}{\alpha r^2 c_s^2} \quad (8)$$

where

$$\Omega_k^2 = \frac{GM}{(r - r_g)^2 r} \quad (9)$$

and r_g is the equal to GM/c^2 and j is the angular momentum of the system.

Solving equation (5) for ε gives a reasonable approximation of the neutrino emission by the disk. By using the following approximations (Vishniac & Wheeler 1996):

$$V_r \sim \frac{\alpha c_s^2}{r \Omega} \quad \text{and} \quad \alpha = \alpha_0 \left(\frac{h}{r}\right)^n \quad (10)$$

where α_0 is a constant and n is a constant of order $3/2$, we find:

$$\varepsilon = \left(\frac{\dot{M}\Omega r^2}{4\pi c_s} \right) \times \left(\frac{\partial\Omega}{\partial r} \right)^2 - \left(\frac{n\dot{M}(GM)^{1/2} c_s^2}{4\pi \Omega hr^{7/2}} \right) \quad (11)$$

MacFadyen & Woosley (1999) estimate a neutrino emissivity due to the pair production process, which will be discussed later, to be about 9×10^{33} ergs $\text{cm}^{-3} \text{s}^{-1}$.

Using the conservation laws of Gammie & Popham (1998) and various parameters from MacFadyen & Woosley's (1999) 14 solar mass helium star model (see Table 2), one can arrive at an estimate of the neutrino emission by solving for ε from equation (27). ε can reach values of 35×10^{33} ergs $\text{cm}^{-3} \text{s}^{-1}$.

r (cm)	10^7
M (solar mass / s)	0.07
ρ (g / cm^3)	10^9
V_r (cm / s)	10^9
Ω (s^{-1})	1000
T (K)	10^{10}
h (cm)	$5 \cdot 10^6$
j (cm^2 / s)	10^{17}

Table 2: Hypernova Model parameters taken from McFadden & Woosley (1999).

Chapter 3

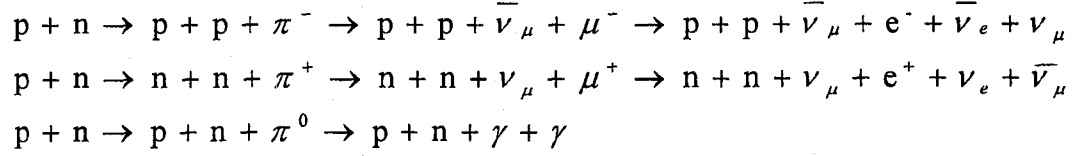
Neutrino Emissivity & Rates

3.1 Neutrino Production in Jets

There are many processes capable of producing neutrinos in the environment inside the accretion disks associated with a hypernova or a stellar object merger with a black hole. Low energy neutrino production will be discussed in detail shortly, but let us first summarize at high-energy processes, such as production of neutrinos in jets of black holes, for completeness.

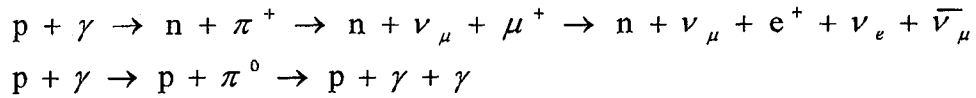
Neutrinos of energies between 2 - 25 GeV should arise from longitudinal decoupling of the neutron and proton flows in jets. That is expected whether or not internal shocks occur, provided a substantial fraction of neutrons are present in the

fireball. A fireball is a jet produced by a black hole and is radiation-dominated rather than matter-dominated. When the total fireball bulk Lorentz factor is greater than or equal to 400 (Bahcall & Meszaros 2000; Meszaros & Rees 2000) the relative neutron and proton drift velocity should approach the speed of light and the inelastic pion production threshold of 140 MeV should be reached. Then the following reactions will be able to take place to produce the neutrinos:



TeV neutrinos are expected to be produced from successful and choked fireballs originating from the hypernova model (Meszaros & Waxman 2001). Those neutrinos should appear as precursors to the successful fireballs and they should be detected even if the fireball is stopped during its passage through a stellar envelope.

Neutrinos of energy greater than 200 TeV are expected from the photo-pion process in p- γ interactions between protons accelerated in shocks and the photons produced by synchrotron emission from electrons during the same shocks (Waxman & Bahcall 1997). The photo-pion process produces the following:



Neutrinos of energy $10^5 - 10^7$ TeV are produced in the initial stage of the

interaction of the fireball with its surrounding gas. Protons are accelerated to high energy in these “reverse” shocks along with newly created low energy optical – UV photons (Waxman 2000). The neutrinos are produced via photo-pion interactions like the reactions listed above.

3.2 Neutrino Production in Accretion Disks

At low energies, quasi-thermal neutrinos of energy 10-30 MeV are associated with stellar collapse, accretion disks, or merger events that trigger the burst (Janka & Ruffert 1996). In terms of the physics of the creation of these neutrinos, there are multiple ways in which they can be generated in these extreme environments. Pair, plasma, recombination, bremsstrahlung, and photo processes are different pathways that produce neutrinos. These theories are based on the Weinberg-Salam theory (Weinberg 1967; Salam 1968) about the electroweak interaction (Itoh & Kohyama 1983). The following processes will be discussed and their relevance for the environments of the accretion disks.

3.2.1 Pair Neutrino Emission

Neutrinos can be created when an electron and a positron interact via the weak interaction which produces either a Z or a $W^{+/-}$ vector boson which then produces a $\nu_{e,\mu,\tau}$ and its corresponding anti-neutrino (Schinder et al. 1987). This process occurs over the

temperature range of $10^9 < T < 10^{11}$ K and density range divided by electron chemical potential $1 < \rho/\mu_e < 10^{14}$ g cm⁻³ (Itoh et al. 1990), and is the dominant process (it contributes over 90% of the total emission) at high temperatures, $T > 10^{10}$ K (Haft et al. 1994).

Itoh et al. (1990) have worked out an accurate fitting formula for the energy loss rate per unit volume per unit time due to the pair neutrino process:

$$Q_{\text{pair}} = \frac{1}{2}[(C_V^2 + C_A^2) + n(C_V'^2 + C_A'^2)] \times \left[1 + \left\{ \frac{(C_V^2 - C_A^2) + n(C_V'^2 - C_A'^2)}{(C_V^2 + C_A^2) + n(C_V'^2 + C_A'^2)} \right\} q_{\text{pair}}(\lambda) \right] g_{\text{pair}}(\lambda) e^{-2/\lambda} F(\lambda) \quad (12)$$

where n is the number of neutrino flavours other than the electron neutrino, $C_i = (\zeta_i^2 + (\zeta_i - 1)^2)^{1/2}$, $C_i' = 1 - C_i$ where $i = V$ or A , $\zeta_V = 1/2 + 2\sin^2\theta_W$, $\zeta_A = 1/2$, $\sin^2\theta_W = 0.2319$ is the Weinberg angle, $\lambda \propto T$, $g(\lambda)$ and $q_{\text{pair}}(\lambda)$ are fitted polynomials derived from the pair interaction, and (Itoh et al. 1990):

$$F(\lambda) = \frac{a_0 + a_1\xi + a_2\xi^2}{\xi^3 + b_1\lambda^{-1} + b_2\lambda^{-2} + b_3\lambda^{-3}} e^{-c\xi} \quad (13)$$

where $\xi \propto \rho/\mu_e$, while λ and the a and b constants are temperature and model dependent. This is the fitting formula that MacFadyen & Woosley (1999) use to estimate the energy loss from their models.

3.2.2 Plasma Neutrino Emission

Plasma neutrinos will be formed when energetic photons with energies greater

than 1 MeV spontaneously produce an electron-positron pair, which then interacts via a Z or W^{+-} vector boson. This, in turn produces a $\nu_{e,\mu,\tau}$ and an anti-neutrino (Schinder et al. 1987). This process occurs over the temperature range of $10^8 < T < 10^{11}$ K and density range $1 < \rho/\mu_e < 10^{14}$ g cm⁻³ (Itoh et al. 1990), and is a dominant factor over the whole temperature range for varying ρ/μ_e values (Haft et al. 1994).

Itoh et al. (1990) have worked out an accurate fitting formula to the energy loss rate per unit volume per unit time due to the plasma neutrino process:

$$Q_{\text{plasma}} = (C_V^2 + nC_V'^2) \times \left(\frac{\rho}{\mu_e} \right)^3 F(\lambda) \quad (14)$$

3.2.3 Recombination Neutrino Emission

Neutrinos are produced in this process when an electron in the continuum state makes a transition to a bound state, thereby emitting a electron neutrino pair (Kohyama et al. 1993). This process occurs over the temperature range of $T < 6 \times 10^9$ K and density range $\rho/\mu_e < 10^6$ g cm⁻³ (Itoh et al. 1990), where the electrons are non-relativistic (Kohyama et al. 1993).

Kohyama et al. (1993) have worked out the energy loss rate per unit volume per unit time due to the recombination neutrino process:

$$Q_{\text{recombination}} = 2 \int \frac{\sigma(\varepsilon_i) \times (\varepsilon_i + I) \times \nu N d^3p}{(2\pi)^3 (e^{(\varepsilon_i - \mu)/kT} + 1)} \quad (15)$$

where σ is the scattering cross section, ε_i is the energy of the initial state of the electron, I is equal to $\frac{1}{2} Z^2 \alpha^2 m_e c^2$ where Z is the charge of the completely ionized atom and α is the fine structure constant, N is the number of the vacant states on the K shell of the atom per unit volume, p is momentum, and μ is the chemical potential parameter.

3.2.4 Bremsstrahlung Neutrino Emission

Energetic nucleons can interact via the electroweak force producing a Z or $W^{+/-}$ vector boson which then produces a $\nu_{e,\mu,\tau}$ and an anti-neutrino (Raffelt 2001). This process occurs over the temperature range of $10^6 < T < 10^9$ K and density range $1 < \rho/\mu_e < 10^9$ g cm⁻³ (Itoh et al. 1990), and dominates in extremely high densities and relatively low temperatures $10^7 < T < 10^8$ K (Munakata et al. 1985).

The neutrino energy loss rate per unit volume per unit time of a single species, nonrelativistic, nondegenerate, thermal nucleon gas can be expressed as (Raffelt 2001):

$$Q_{\text{bremsstrahlung}} = n_B \left(\frac{C_A G_F}{(2\pi)^3} \right)^2 \int (\varepsilon_1 + \varepsilon_2) \times (3 - \cos\theta) \times S(\omega, k) d^3k_1 d^3k_2 \quad (16)$$

where G_F is the Fermi coupling constant and is equal to $1.02679 \times 10^{-5} m_e^{-2}$, $S(\omega, k)$ is a function that describes the axial-current neutrino-nucleon scattering, θ is the scattering angle, ε_1 and ε_2 are the energies of the emitted neutrinos, and k_1 and k_2 are their

respective momenta.

3.2.5 Photo Neutrino Emission

Neutrino emission due to the photo process is due to photons interacting with an electron or a positron which then produce a Z or $W^{+/-}$ vector boson that produces a $\nu_{e,\mu,\tau}$ and an anti-neutrino (Schinder et al. 1987). This process occurs over the temperature range of $10^7 < T < 10^{11}$ K and density range $1 < \rho/\mu_e < 10^{14}$ g cm $^{-3}$ (Itoh et al. 1990), and is a dominant neutrino production process over the temperature range $10^{7.5} < T < 10^9$ K and density range $10^3 < \rho/\mu_e < 10^6$ g cm $^{-3}$ (Haft et al. 1994).

Itoh et al. (1990) have worked out an accurate fitting formula for the energy loss rate per unit volume per unit time due to the photo neutrino process:

$$Q_{\text{photo}} = \frac{1}{2} \times [(C_V^2 + C_A^2) + n(C_V'^2 + C_A'^2)] \times \left[1 + \frac{(C_V^2 - C_A^2) + n(C_V'^2 - C_A'^2)}{(C_V^2 + C_A^2) + n(C_V'^2 + C_A'^2)} \right] q_{\text{photo}}(\lambda) F(\lambda) \quad (17)$$

where $q_{\text{photo}}(\lambda)$ is a fitted polynomial derived from the photo interaction.

A detailed derivation for the emissivity from the photo process in the Fermi theory of the electroweak interaction is given in Beaudet, Petrosian, and Salpeter (1967), while the derivation is given in Dicus (1973). The emissivity is given by:

$$Q_{\text{photo}} = \frac{1}{2^4 (2\pi)^9} \int_0^\infty \frac{p^2 dp}{E} f_e(E) \int_0^\infty \frac{k^2 dk}{\omega} f_\gamma(\omega) \int \frac{d^3 p'}{E'} [1 - f_e(E')] \int_{-1}^1 dw \int \frac{d^3 q}{q_0} \int \frac{d^3 q'}{q'_0} \times \mathcal{G} \quad (18)$$

and

$$\mathcal{G} = \delta(E + \omega - E' - q_0 - q'_0) \times \delta^3(\vec{p} + \vec{k} - \vec{p}' - \vec{q} - \vec{q}') \times (E + \omega - E') \times \sum_{s,\varepsilon} |M|^2 \quad (19)$$

where $p = (E, \mathbf{p})$ is the four momentum of the incoming electron, $p' = (E', \mathbf{p}')$ is the four momentum of the final electron, $k = (\omega, \mathbf{k})$ is the four momentum of the incoming photon, $q = (q_0, \mathbf{q})$ is the four momentum of the emitted neutrino, $q' = (q'_0, \mathbf{q}')$ is the four momentum of the emitted anti-neutrino, $f_e(E)$ is the Fermi electron distribution function and is equal to $[e^{(E-\mu)/kT} + 1]^{-1}$, $f_\gamma(\omega)$ is the photon distribution function and it is equal to $[e^{\omega/kT} - 1]^{-1}$, and $w = \cos(\mathbf{p} \cdot \mathbf{k})$.

The $\sum |M|^2$ term is the scattering amplitude and is calculated from the matrix element given in Dicus (1973) and is based on the interaction of interest:

$$\sum_{s,\varepsilon} |M|^2 = \left(\frac{e^2 g^2}{64 m_W^4} \right) \times \text{Tr}[\not{q} \gamma_\alpha (1 - \gamma_5) (-\not{q}') (1 + \gamma_5) \gamma_\beta] \times \text{Tr}[A \times B] \quad (20)$$

where

$$A = (\not{p}' + m) \left[\frac{\gamma^\alpha (C_V - C_A \gamma_5) (Q_1 + m) \not{\xi}}{\beta_1} + \frac{\not{\xi} (Q_2 + m) \gamma^\alpha (C_V - C_A \gamma_5)}{\beta_2} \right] \quad (21)$$

and

$$B = (\not{p} + m) \left[\frac{(C_V + C_A \gamma_5) \gamma^\beta (Q_2 + m) \not{\xi}}{\beta_2} + \frac{\not{\xi} (Q_1 + m) (C_V + C_A \gamma_5) \gamma^\beta}{\beta_1} \right] \quad (22)$$

where $g = (hc\alpha/2\pi)^2$, α is the fine structure constant, m_W is the mass of the W vector boson which equals 82 GeV, $m = m_e$, $Q_1 = p + k$, $Q_2 = p' - k$, $\beta_1 = (p + k)^2 - m^2 = 2k \cdot p +$

$$\omega_0^2, \text{ and } \beta_2 = (\mathbf{p}' - \mathbf{k})^2 - m^2 = -2\mathbf{k} \cdot \mathbf{p}' + \omega_0^2.$$

When summing over the photon polarization states, ξ , Schinder et al. (1987) have chosen $\xi \cdot \xi = -1$ and ξ^μ is equal to $(0, \xi)$ in the rest frame of the initial electron. In this frame:

$$(\xi \cdot \mathbf{p}) = 0 \quad \sum_{\xi} (\xi \cdot \mathbf{p}') = |\mathbf{p}'|^2 - \frac{(\bar{\mathbf{p}}' \cdot \bar{\mathbf{k}})^2}{|\bar{\mathbf{k}}|^2} \quad (23)$$

3.3 Neutrino Detection

Super-Kamiokande (Super-K) located in Gifu Prefecture, Japan, is a detector of neutrinos that have energies on the order of a few MeV to GeV. This detector is used for detecting solar neutrinos, supernovae neutrinos, atmospheric neutrinos, proton decay, monopoles, dark matter, and neutrino oscillation using day/night and seasonal variation of the solar neutrino flux. Construction of Super-K was started in 1991 and was completed at the end of 1995 with data taking starting on April 1, 1996. The detector is located 1000 m underground in the Kamioka mine and compared to ground level, the detector receives a cosmic ray muon intensity that is reduced by about one in one hundred thousand.

The detector uses fifty thousand tons of pure water in a cylindrical tank and has a diameter of 39.3 m and a height of 41.4 m. The engineers also constructed an outer and

inner detector, the outer detector is used to discriminate entering cosmic ray muons and is used as a buffer to keep radiation emitted and neutrons by the surrounding rock and walls from entering the inner volume. The outer detector uses 1885 eight inch PMTs while the inner section uses 11146 twenty inch PMTs that are placed at intervals of 70 cm. The ratio of PMT area to total area is about 40.41%. Super-K uses Cerenkov light produced in the interaction of neutrinos and protons or neutrons from the water or electron neutrino scattering. In terms of energy resolution Super-K can detect neutrinos with energies of 1 GeV at 2.5% and at 10 MeV at 16% with an energy threshold of 5 MeV.

Other neutrino detectors are Kamiokande I in Japan, the Russian-Italian experiment in the Mont Blanc tunnel, the Baksan experiment in the USSR, the IMB experiment in the USA, and the Sudbury Neutrino Observatory (SNO) located in Ontario, Canada.

3.4 Summary

Kamiokande I, IMB, Baksan, and Mont Blanc were able to detect neutrinos from SN 1987A, which was located in the Large Magellentic Cloud (LMC) 50 kpc away. Mechanisms that produce a supernova range from a bounce shock off of a neutron star to a black hole forming before the shock escapes the star and the jets of the black hole blowing up the star in an axial-driven hypernova. The detection of these neutrinos gave

astronomers insights into the mechanism that produced this supernova. This is discussed in detail in Chapter 5.

In the environment of a hypernova accretion disk, temperatures can range from 10^8 K to 10^{11} K and pair and photo neutrino production processes should dominate and to a lesser extent the plasma process is also present. Their emissivity and rates are given in table 3 with their corresponding temperatures and are taken from Schinder et al. (1987).

Process	Temp. (K)	Emissivity (ergs/cm ³ /s)	Rates (1/cm ³ /s)	Temp. (K)	Emissivity (ergs/cm ³ /s)	Rates (1/cm ³ /s)
Plasma	10^8	10^7	10^{14}	10^{11}	10^{27}	10^{31}
Pair	10^9	10^{14}	10^{17}	10^{11}	10^{34}	10^{37}
Photo	10^9	10^{12}	10^{19}	10^{11}	10^{31}	10^{35}

Table 3: Emissivity and Rates of neutrinos at their corresponding temperatures.

Chapter 4

Results & Conclusions

4.1 Monte Carlo Method

The Monte Carlo method, developed in the 1940s at the Los Alamos National Laboratory, can estimate the area under curves by using random numbers or co-ordinates selected from a generating function. This method is employed when finite multi-dimensional integrals cannot be solved using analytic methods. For each dimension, random numbers are selected for independent variables and scaled accordingly, then plugged into the function that is being integrated. This process is repeated for an appropriate number of turns, with each value of the function being added to the sum of the others. The value of the integral can be recovered with (Kalos & Whitlock 1986):

$$\int f dV \approx V \times \langle f \rangle \tag{24}$$

with an uncertainty of (Kalos & Whitlock 1986):

$$V \times \left(\frac{\langle f^2 \rangle - \langle f \rangle^2}{N} \right)^{1/2} \quad (25)$$

where f is the function of integration, N is the number of turns for which the process is repeated, and V is a minimized multi-dimensional volume that encompasses the function.

4.2 Results

The parameters of interest, taken from Table 2, are the temperature, electron chemical potential, and the radius within which most of the neutrinos are created. MacFadyen & Woosley (1999) don't explicitly give the chemical potential value, however it can be calculated from the equilibrium distribution of the density given by (Kolb & Turner 1990):

$$\rho = \frac{g}{2\pi^2} \int_m^\infty \frac{(E^2 - m^2)^{1/2}}{\exp[(E - \mu)/T] + 1} E^2 dE \quad (26)$$

where g denotes the number of internal degrees of freedom, m is the rest mass of the electron, and E^2 is the square of the relativistic energy equal to $|\mathbf{p}|^2 + m^2$. The values of the density and temperature are given, and the value of the chemical potential can be calculated through a shooting algorithm. We convert from natural units of ergs^4 to g/cm^3 by multiplying the integral by $1/[(h/2\pi)^3 c^5]$.

The calculation for the emissivity can be completed after a value for the electron chemical potential is found. The latter is done by creating a Monte Carlo code, reproduced in Appendix A, to calculate equation (26). The value of the density, 10^9 g cm^{-3} , and temperature, 10^{10} K , are given and, the value of the chemical potential can be calculated. A chemical potential $\mu_e = 2.02 \times 10^7 \text{ eV}$ results in a value for the density of $(1.001 \pm 0.002) \times 10^9 \text{ g/cm}^3$.

Since the photo process is a dominate mechanism in the disk of a hypernova it is important to calculate its emissivity. Q_{photo} (equation 18) can be calculated after eliminating two of the integrals by using the two delta functions found in equation (19). The momentum conservation delta function, $\mathbf{p}' = \mathbf{p} + \mathbf{k} - \mathbf{q} - \mathbf{q}'$, removes the \mathbf{p}' integral. The energy conservation delta function, $\omega = E' + q_0 + q_0' - E$, coupled with $\omega = kc$ implies that:

$$k = \frac{q_0^2 + 2q_0(q_0' - E) + q_0'^2 - 2Eq_0' - m_e^2 - (\bar{q}' - \bar{p} + \bar{q}) + E^2}{2[q_0 + q_0' - (\bar{q} + \bar{q}' - \bar{p}) - E]} \quad (27)$$

which then removes the k integral.

One can also eliminate the neutrino (q) and anti-neutrino (q') integrals by calculating:

$$\frac{\partial Q_{\text{photo}}}{\partial q^3 \partial q'^3} = \frac{1}{2^4 (2\pi)^9} \int_{-1}^1 dw \int_0^\infty p^2 dp f_e(E) k^2 f_\gamma(\omega) [1 - f_e(E')] \frac{(E + \omega - E')}{E \cdot \omega \cdot E' \cdot q_0 \cdot q_0'} \sum_{s,\epsilon} |M|^2 \quad (28)$$

Q_{photo} is then recovered by integrating over the neutrino and anti-neutrinos

energies over equation (28). This can be seen in the following:

$$Q_{\text{photo}} = 4\pi \int_0^{\infty} \bar{q}^2 d\bar{q} \int_0^{\infty} 2\pi \bar{q}'^2 d\bar{q}' \int \sin(\theta_{q,q'}) d\theta \frac{\partial Q_{\text{photo}}}{\partial q^3 \partial q'^3} \quad (29)$$

We convert the natural units of $\text{ergs}^7 \text{cm}^2$ to $\text{ergs}/\text{cm}^3/\text{s}$ by multiplying the integral by $1/[(h/2\pi)^6 c^5]$.

To calculate the emissivity, equation (29), of neutrinos from the photo process a Monte Carlo program is written, reproduced in Appendix B. The input variables into the code are the temperature and electron chemical potential. The incoming electron, neutrino, and anti-neutrino momentum variables are selected from a random number generator and are scaled according to their specific ranges and placed into the function. The angles of the incoming electron, neutrino, anti-neutrino momentum, and photon wave number are also selected from a generating function. The corresponding rate at which neutrinos are leaving the disk is found by removing the $(E + \omega - E')$ expression from equation (28). The same code is used for this calculation.

Using the Monte Carlo code listed in Appendix B gives values of emissivity and rates for volumes of 0 to 10^9 eV for the incoming electron momentum and 2×10^6 to 10^7 eV for the neutrino and anti-neutrino. For these volumes, an emissivity of $(8.7 \pm 0.1) \times 10^{21} \text{ ergs cm}^{-3} \text{ sec}^{-1}$ is found. A rate of emission $(8.6 \pm 0.1) \times 10^{26} \text{ cm}^{-3} \text{ sec}^{-1}$ is given. If one divides the emissivity by the rate and convert ergs to eV, an average energy of the emitted neutrino is calculated to be $(6.2 \pm 0.2) \times 10^6$ eV.

For volumes of 0 to 10^{10} eV for the incoming electron momentum and 10^6 to 1.5×10^7 eV for the neutrino and anti-neutrino momentum an emissivity of $(7.0 \pm 0.2) \times 10^{21}$ ergs $\text{cm}^{-3} \text{sec}^{-1}$ is given from the code. A rate of $(7.3 \pm 0.2) \times 10^{26} \text{cm}^{-3} \text{sec}^{-1}$ is also given. The average energy of the emitted neutrinos is $(6.0 \pm 0.3) \times 10^6$ eV.

The photo emissivity and rate from Schinder et al. (1987) is written out explicitly in the appendix to their paper. They start with equation (18), however they make approximations to their scattering amplitude (equation 20) and first integrate over the neutrino and anti-neutrino energy. They then use this equation, which they call equation (6) in their paper, to calculate the photo emissivity and rate for various densities and temperatures using the Monte Carlo method. We have performed a more complete and robust calculation in this work using a complete scattering amplitude.

Their results for the photo emissivity for a temperature of 10^{10} K, density of 10^9 g/cm^3 , and a chemical potential of 10^7 eV are between $6-9 \times 10^{21}$ ergs $\text{cm}^{-3} \text{s}^{-1}$. Similarly for the rate of photo neutrinos, they find a result of $6-9 \times 10^{26} \text{cm}^{-3} \text{s}^{-1}$ with an average neutrino energy between 5.5-6 MeV. A comparison between the results from the work done in this thesis and Schinder et al. (1987) can be seen in Table 4.

4.3 Conclusions

The results from calculating the emissivity and the rate using the complete

Neutrino Properties	Run Number 1	Run Number 2	Schinder et al. (1987)
Emissivity (ergs cm ⁻³ sec ⁻¹)	(8.7 +/- 0.1)×10 ²¹	(7.0 +/- 0.2)×10 ²¹	6-9×10 ²¹
Rates (cm ⁻³ sec ⁻¹)	(8.6 +/- 0.1)×10 ²⁶	(7.3 +/- 0.2)×10 ²⁶	6-9×10 ²⁶
Neutrino Energy (MeV)	(6.2 +/- 0.2)	(6.0 +/- 0.3)	5.5-6.0

Table 4: Comparison of the results of this work to those of Schinder et al. (1987).

scattering amplitude for various limits of the integrals, and using the Monte Carlo method yields similar results to those of Schinder et al. (1987) for the emissivity, rate, and average neutrino energy for the photo process. Therefore I can infer that my results are correct.

I find a weak departure for the emissivity and rate for these neutrinos on the limits of integration. However, the average energy for the neutrinos is the same. This can be accounted for by the fact that the parameters I used from MacFadyen & Woosley's (1999) model result in the conservation of energy. The neutrinos released from a radius 10⁷ cm, which has a temperature of 10¹⁰ K and density of 10⁹ g/cm³, produces neutrinos of energy on the order of 6 MeV. It is likely that the departure is an artifact of the tails of the Fermi/Bose distributions over the volume of integration.

Detectors such as Super-Kamiokande would be able to detect such neutrinos

since their lower limit of detection is 5 MeV. However, at distances of redshift one, these neutrinos wouldn't be distinguishable as thermal accretion disk neutrinos because solar neutrinos, specifically ^8B neutrinos from the sun, have the same energies and the disk neutrinos would be thought of as such.

Chapter 5

Supernova 1987A

5.1 Neutrino Detection

If a hypernova did occur within our galaxy, neutrinos from the explosion would be detected. These would be thermal accretion disk neutrinos, with a large number detected on a short timescale of ten seconds, along with visual observation of the hypernova. A possible example is SN 1987A where 3 neutrino detectors saw a total of 25 neutrino events within thirty seconds. A fourth detector also saw 5 neutrino events four and a half hours before the actual supernova explosion.

This fourth detector was the Mont Blanc experiment and it detected neutrinos with an energy range of 6-7.8 MeV. Saha and Chattopadhyay (1991) state that their

detection of these neutrinos, correlated with the supernova, have been disputed. Aglietta et al. (1987) have shown that Mont Blanc neutrino detection is correlated with gravitational-wave data recorded in Rome and Maryland, while Saha and Chattopadhyay (1991) claim that the Mont Blanc neutrino signal was real with the same eleven milli-second period that the other neutrino detectors see. The authors state that the eleven milli-second period is consistent with a rotational period of a neutron star core.

Hillebrandt et al. (1987) suggests that the proto-neutron star collapsed to form a neutron star at the time were Mont Blanc detected their neutrino burst. Four and a half hours later, as this information was traveling through the star, the neutron star accreted enough material to form a black hole. At this point matter from the star fell into the last stable orbit around the black hole and the star blew up in an axial-driven supernova or hypernova.

Kamiokande I, IMB, and Baksan were the three other detectors that saw neutrinos coincident with the visual observations of the supernova explosion. Baksan detected five neutrinos with an energy range of 12 to 23.3 MeV. Kamiokande detected twelve events with an energy range of 6.3 to 35.4 MeV and IMB saw eight neutrinos with an energy range of 19 to 39 MeV. Kamiokande was the only detector with information about the direction of the neutrinos. The angles with respect to the LMC range from 15 to 135 degrees. Burrows & Lattimer (1987) suggest that since most of the events do not point towards the LMC and then none of the events were neutrino-electron scattering events, and had to have been anti-neutrino absorption events. Burrows & Lattimer (1987) state that this implies that these neutrinos must have come from the

deleptonization of the neutron star core and the supernova in question must have occurred in the normal fashion. Haubold et al. (1988) point out that this is not necessary since neutrinos from an accretion disk should produce the same number of neutrinos and anti-neutrinos and that the cross-section for neutrino-electron scattering is a hundred times less than anti-neutrino absorption (Burrows & Lattimer 1987). Therefore the detectors are biased towards detecting anti-neutrino absorption and this result alone can not rule out an axial-driven supernova.

5.2 Discussion

Burrows & Lattimer (1987) plot the integrated Kamiokande I and IMB event rate per 0.25 second bin. They find a sharp rise in events in the first second with a steady climb of events for the remaining twelve seconds. They state that the data can be fit to supernova models with and without convection of neutrinos to the stalled shock. That seems odd since most models of neutrino emission from supernovae have a sharp rise with the deleptonization of the neutron star, then a slow decline of neutrino flux as the neutrinos leak out of the neutrino-sphere. They state that they cannot rule out the possibility that a black hole formed and caused the neutrino events. They go on to state that it is hard to reconcile seeing neutrinos for such a long time-scale with production by a black hole, which should have a neutrino emission that stops after a few seconds.

In the hypernova model, matter falls into the last stable orbit of the black hole

over a period of fifteen seconds, as seen in MacFadyen & Woosley (1999) models. Matter is accreted onto the black hole where neutrino emission is present, which helps form the jets that eventually break free from the star. I believe that the integrated Kamiokande I and IMB data that Burrow & Lattimer (1987) present is characteristic of thermal accretion disk neutrinos because of the slow rise of neutrinos rather than a slow fall off. The sharp rise is due to the creation of the black hole and the onset of accretion. As time goes on more matter is being pulled onto the black hole disk creating a rise in the production of neutrinos.

The precursor of SN 1987A has been suggested to be a blue supergiant (Prantzos et al. 1988) with an initial mass of 15 to 20 solar masses. The helium core of the star had to have been at least 6 solar masses to explain the observed luminosity (Prantzos et al. 1988). Prantzos et al. (1988) state the mass of the helium star was in the range of 6.3 to 7 solar masses. MacFadyen & Woosley's (1999) two models for an axial-driven supernova had helium cores of 9 and 14 solar masses.

Constant monitoring by fast photometry has not shown that the remnant of SN 1987A is a pulsar, and is more likely the remnant is a black hole (Haubold et al. 1988). Observations of the supernova remnant imply that it is axially-symmetric and not spherically-symmetric which would be the case for a normal supernova.

Wang et al. (2002) has observed SN 1987A with the Hubble Space Telescope using the F439W filter on 2000 June 11. They state that the images show the remnant to

be asymmetric and substantially bipolar. With this observed asymmetry, it is highly unlikely that the normal core bounce mechanism could reproduce this geometry (Wang et al. 2002). Therefore, Wang et al. (2002) conclude that a jet-driven model for the cause of this remnant seems probable. However, the exact mechanism for the production of the jets is unclear. Models range from a magnetized rotating proto-neutron star (Symbalisty 1984), neutrino heating from a proto-neutron star (Tohline et al. 1980), asymmetries associated with neutrino flow (Fryer & Heger 2000), and a hypernova (MacFadyen & Woosley 1999; Nagataki 2000).

The possibility that SN 1987A occurred via the same mechanism of the MacFadyen & Woosley (1999) models experienced, which they call a hypernova, exists. Therefore, the thermal accretion disk neutrinos that I have studied here may, in fact, have been detected from SN 1987A.

Appendix A

Code for Determining the Electron Chemical Potential

The code is written for a Fortran 77 compiler. A Monté Carlo method is used to evaluate equation (26). Values of density $\sim 10^9$ g/cm³ and temperature $\sim 10^{10}$ K at $r \sim 10^7$ cm are given in MacFadyen & Woosley (1999), not the electron chemical potential which is also needed.

- Section 1: Defining the Variables
- Section 2: Reading the Seed Variables
- Section 3: Declaring the Variables' Value
- Section 4: Finding the Average of the Function
- Section 5: Calculating the Mean and its Uncertainty
- Section 6: Displaying Results
- Section 7: Uniform Random Number Generator between 0 & 1

CC
CC

PROGRAM Determining the Electron Chemical Potential

CC

C SECTION 1 - "Defining the Variables"

C Variables in the "do loop"

Integer N, I

C Random number variable

Real x

C Energy Variable

Real*8 e

C Variable for pi=3.14159

Real*8 p

C Electron mass

Real*8 m

C Internal degrees of Freedom of the Electron (Spin)

Real*8 g

C Temperature ~ 10**10 Kelvins

Real*8 kt

C Density and Uncertainty ~ 10**9 g/cm**3

Real*8 Density ~ 10**9 g/cm**3

C Chemical Potential: need 2.02*10**7

Real*8 mu

C Volume of integral

Real*8 vol, a, b

C Fuction of integration

Real*8 sum, sumsq, f

C Unit conversion variables

Real*8 five, c, hbar, con, ergs, units

C End of Section 1

CC

CC

C SECTION 2 - "Reading the Seed Variables"

```
print *, 'Enter a random number: e energy'  
read *, x
```

C END OF SECTION 2

CC

C SECTION 3 - "Declaring the Variables' Value"

```
N=1000000  
p=3.14159  
g=2
```

C "All Units in eV"

```
m= .511*10**6  
five= 1.d0/(10**5)  
mu= 2.02*1.d2/five
```

C "Conversion of Kelvin to eV"

```
kt= (8.62*10**9)/(10**4)
```

C "Volume of the integral"

```
a= 5*10**7  
b= 10**0  
vol= a*b - m
```

```
sum= 0  
sumsq= 0
```

C END OF SECTION 3

CC

C SECTION 4 - "Start of the Do Loop"
C - "Finding the Average of the Density"

DO 10 I = 1, N

call random(x)

e= vol*x + m

C "Conversion of Units: eV -> ergs"

ergs= 1.602*five*five/(100)

C "Have ergs**4 -> Need g/cm**3 so multi. by 1/(hbar**3*c**5)"

hbar= 6.58*five*five*five/10

c= 3*(five*five)**(-1)

con= 1.d0/(hbar**3*c**5)

units= ergs*con

f= (g/(2*p*p))*e*e*SQRT(e*e-m*m)/(exp((e-mu)/kt) + 1)

sum= sum + f*units

sumsq= sumsq + (f*units)**2

Open (20, file='chemical.txt', status='unknown')

Write (20,*) e, f

10 continue

C END OF SECTION 4

CC

C SECTION 5 - Calculating the Mean & Uncertainty"

C From equations 22 & 23

```
density= vol*sum/dble(N)
uncertain= vol*SQRT((sumsq/dble(N) - (sum/dble(N))**2)/dble(N))
```

C END OF SECTION 5

CC

C SECTION 6 - "Displaying Results"

```
print *, 'Density'
print *, density
print *, 'Uncertainty'
print *, uncertain
print *, 'Energy'
print *, e
print *, 'Temperature'
print *, kt
print *, 'Chemical Potential'
print *, mu
```

```
write (20,*) density
```

C "END OF PROGRAM Determining the Electron Chemical Potential"

```
end
```

C END OF SECTION 6

CC

CC

C SECTION 7 - "Random Number Generator 0 -> 1"

SUBROUTINE random (rannum)

integer n, const1
real rannum, const2
parameter (const1 = 2147483647, const2 = .4656613E-9)
save
data n /0/

if (n .eq. 0) n = int(rannum)
n = n * 65539
if (n .lt. 0) n = (n + 1) + const1
rannum = n * const2

end

C END OF SECTION 7

CC
CC

Appendix B

Code for the Photo Neutrino Emissivity/Rates

The code is written for a Fortran 77 compiler. A Monté Carlo method is used to evaluate equation (29), the photo neutrino emissivity from an accretion disk produced by a hypernova. Values for the constants are taken from MacFadyen & Woosley (1999).

Section 1: Defining the Variables

Section 2: Reading the Seed Variables

Section 3: Declaring the Variables' Value

Section 4: Finding the Average of the Function / First "Do Loop"

Section 5: Finding the Average of the Function / Nested "Do Loop"

Section 5.1: Plasma Frequency Calculation

Section 5.2: Dot Products in the Amplitude

Section 5.3: First Part of the Amplitude

Section 5.4: Second Part of the Amplitude

Section 5.5: The Final Form of the Amplitude

Section 5.6: Addition of the Function and the Function Squared

Section 6: Calculating the dQ_{photo} and its Uncertainty

Section 6.1: Addition of the Function and function Squared

Section 7: Calculating the Q_{photo} and its Uncertainty

Section 8: Displaying Results

Section 9: Uniform Random Number Generator 0 -> 1

CC
CC

PROGRAM Photo Neutrino Emissivity

CC

C SECTION 1 - "Defining the Variables"

C Variables for the "do loop"

Integer N, I, nn, ii, nnn, iii

C Momentum for the initial electron

Real p

C Energy for the initial electron

Real*8 e

C Energy and momentum for the final electron

Real*8 ep, pp

C Energy and momentum for the photon

Real*8 w, k

C Energy and momentum for the emitted neutrino

Real*8 qo, q

C Energy and momentum for the emitted anti-neutrino

Real*8 qop, qp

C Variables needed to define k

Real*8 ka, kb

C Angle between p and k

Real u

C Angle between q and p (q defines the z-axis)

Real*8 oqp

C Angle between q and qp (other angles relative to q)

Real*8 oqqp

C Angle between q and k

Real*8 oqk

C Angle between qp and k

Real*8 oqpk

C Angle between p and qp

Real*8 phi

C Variables for cos(angle)
 Real*8 ha, hb, hc, hd
 C Fermi dist. for the initial & final electron
 Real*8 fe, fep
 C Fermi distribution function for the photon
 Real*8 fg
 C Temperature & chemical potential
 Real*8 kt, mu, five
 C Constant = $1/(2^{**13} * 3.14159^{**9})$
 Real*8 consta

 C Random # between zero and one, a -> p while b -> u
 Real a, b
 C Volume of integration: aa vol of p, ab vol of u
 Real*8 vol, aa, ab
 C Function of integr. plus function squared
 Real*8 f, fsquared, equation, y, z
 C Qphoto and uncertainty
 Real*8 Qphoto, dQphoto, uncertainty, volqphoto, vq, vqp

 C Speed of light, electron mass, W vector boson mass
 Real*8 c, m, mw, mwa

 C Plasma frequency
 Real*8 woa, wo
 C Plasma functions
 Real*8 g, ga, gb, gc, gd
 C Fine structure constant
 Real*8 alpha, lambda
 C Variables of interest
 Real xxa, xa, xxb, xb, xxc, xc, xxd, xd
 C Const. for plasma frequency calculations
 Real*8 suma, sumb, sumc, sumd, vola, volb, volc, vold
 C Const. for plasma frequency calculations
 Real*8 v

 C Amplitude
 Real*8 mm, mma, mmb, mmaa, mmab, mmac, mmba, mmbb, mmbc
 C Constants in the amplitude
 Real*8 ccv, cca, cv, ca, ba, bb, s, ss, gg
 C Constants in the amplitude
 Real*8 qa, qae, qb, qbe

 C Constant
 Real*8 constb, hbar

C Variables in the amplitude; Term mma
 Real*8 taa, tab, tac, tad, tae, taf, ta, tba, tbb, tbc, tb
 C Variables in the amplitude; Term mma
 Real*8 tca, tcb, tcc, tc, tda, tdb, tdc, td
 C Variables in the amplitude; Term mma
 Real*8 tea, teb, tec, ted, tee, tef, teg, teh, tei, tej, tek
 C Variables in the amplitude; Term mma
 Real*8 tel, tem, ten, teo, tep, teq, ter, tes, tet, teu, tev
 C Variables in the amplitude; Term mma
 Real*8 tew, tex, tey, tez, teza, tezb, tezc, tezd, teze, tezf
 C Variables in the amplitude; Term mma
 Real*8 tezg, teaa, tebb, tecc, te
 C Variables in the amplitude; Term mma
 Real*8 tfa, tfb, tfc, tfd, tfe, tff, tfg, tfh, tfi, tfj
 C Variables in the amplitude; Term mma
 Real*8 tfk, tfl, tfm, tfn, tfo, tfp, tfq, tfr, tfs, tft, tfu
 C Variables in the amplitude; Term mma
 Real*8 tfv, tfw, tfx, tfy, tfz, tfza, tfzb, tfzc, tfzd, tfze
 C Variables in the amplitude; Term mma
 Real*8 tfzf, tfzg, tfaa, tfbb, tfcc, tf
 C Variables in the amplitude; Term mma
 Real*8 tga, tgb, tgc, tgd, tge, tgf, tg
 C Variables in the amplitude; Term mma
 Real*8 tha, thb, thc, thd, the, thf, th, tia, tib, tic, ti
 C Variables in the amplitude; Term mma
 Real*8 tja, tjb, tjc, tj, tka, tkb, tkc, tk
 C Variables in the amplitude; Term mma
 Real*8 tla, tlb, tlc, tld, tle, tlf, tlg, tlh, tli, tlj
 C Variables in the amplitude; Term mma
 Real*8 tlk, tll, tlm, tln, tlo, tlp, tlq, tlr, tls, tlt, tlu
 C Variables in the amplitude; Term mma
 Real*8 tlv, tlw, tlx, tly, tlz, tlza, tlaa, tlbb, tlcc, tl
 C Variables in the amplitude; Term mma
 Real*8 tma, tmb, tmc, tm, tna, tnb, tnc, tn, toa, tob, toc, to

 C Variables in the amplitude; Term mmb
 Real*8 raa, rab, rac, ra, rba, rbb, rbc, rb, rca, rcb, rcc, rc
 C Variables in the amplitude; Term mmb
 Real*8 rda, rdb, rdc, rd, rea, reb, rec, red, ree, ref, re
 C Variables in the amplitude; Term mmb
 Real*8 rfa, rfb, rfc, rf, rga, rgb, rgc, rg
 C Variables in the amplitude; Term mmb
 Real*8 rha, rhb, rhc, rhd, rhe, rhf, rh

C Variables in the amplitude; Term mmb
 Real*8 ria, rib, ric, rid, rie, rif, ri, rja, rjb, rjc, rj
 C Variables in the amplitude; Term mmb
 Real*8 rka, rkb, rkc, rk, rla, rib, rlc, rld, rle, rlf, rl
 C Variables in the amplitude; Term mmb
 Real*8 rma, rmb, rmc, rmd, rme, rmf, rm
 C Variables in the amplitude; Term mmb
 Real*8 rna, rnb, rnc, rnd, rne, rnf, rn
 C Variables in the amplitude; Term mmb
 Real*8 roa, rob, roc, ro, rpa, rpb, rpc, rp

 C Dot Product Variables
 Real*8 pqa, pqb, ppqa, ppqb, ppp, qap, qapp, qbp, qbpb, qqp
 C Dot Product Variables
 Real*8 qaqa, qaqb, qaeqa, qbqa, qbqb, qbeqb, qqq, eqaeqb
 C Dot Product Variables
 Real*8 eqaeq, eppeqb, eppeq, eqeqb, eqeqp, eppeqb, eqaeqb
 C Dot Product Variables
 Real*8 eppeqa, eqaeqa, eqbeq, eqbeqp, eppep, epeqb, epeqa
 C Dot Products
 Real*8 kq, kqp, kpp, ppq, ppqp, pppp

 C Unit conversions.
 Real*8 one, two, units, ergs, con

 C Random number variable for q
 Real qaaa
 C Random number variable for qp
 Real qpaa
 C Function and uncertainty
 Real*8 ff, ffsq, uncert, uncerta

 C Volume of angle of q & qp
 Real*8 voloqqp, voloqp, volphi, voloqk, voloqpk

 C Random number for angle
 Real oqqpa, oqpa, oqka, oqpka, phia

 C END OF SECTION 1

CC

CC

C SECTION 2 - "Reading Seed Variables"

```
print *, 'Enter a random number: p momentum'  
read *, a  
print *, 'Enter a random number: q momentum'  
read *, qa  
print *, 'Enter a random number: qp momentum'  
read *, qp  
print *, 'Enter a random number: w=u angle between p and k'  
read *, b  
print *, 'Enter a random number: angle between q & qp'  
read *, oqpa  
print *, 'Enter a random number: angle between q & p'  
read *, oq  
print *, 'Enter a random number: angle between q & k'  
read *, oqk  
print *, 'Enter a random number: angle between k & qp'  
read *, oqpk  
print *, 'Enter a random number: 2nd angle between p & qp'  
read *, phi  
print *, 'Enter a random number: xa'  
read *, xa  
print *, 'Enter a random number: xb'  
read *, xb  
print *, 'Enter a random number: xc'  
read *, xc  
print *, 'Enter a random number: xd'  
read *, xd
```

C END OF SECTION 2

CC

C SECTION 3 - "Declaring the Variables' Value"

```
N= 10000  
nnn= 10000
```

C "All units of variables are in eV"

m= .511*10**6
mwa= 82
mw= mwa*10**9

consta= 1.d0/(2**13*3.14159**9)

five= 1.d0/10**5
hbar= 6.58*five**3/10
c= 3*1.d0/five**2
alpha= 1.d0/137
constb= -4*0.2319*(hbar*c*alpha)**2/(64*mw**4)

cca= 0.5
ccv= 0.5+2*(0.2319)
ca= SQRT((cca**2)+2*(cca-1)**2)
cv= SQRT((ccv**2)+2*(ccv-1)**2)

C "Temperature & Chemical Potential"

mu= 2.02*100/five
kt= (8.62*10**9)/(10**4)

C "Volumes of the integral"

one= 10**9
aa= one-0
ab= 2
vol= aa*ab

C "The neutrino & anti-neutrino momentum volumes"

vq= 10*10**6-2*10**6
vqp= 10*10**6-2*10**6
volqphoto= vq*vqp

C "Volumes of the angles"

voloqqp= 3.14159-0
voloqp= 3.14159-0
volphi= 2*3.14159-0
voloqk= 3.14159-0
voloqpk= 3.14159-0

C "Zeroing functions"

ff= 0
ffsq= 0

C END OF SECTION 3

CC

C SECTION 4 - "Start of the Do Loop"
C - "Finding the Average of the Function"

DO 1000 iii = 1, nnn

print *, iii

C "Zeroing functions"

f= 0
fsquared= 0

CC

C SECTION 5 - "Start of the Do Loop"
C - "Finding the Average of the Function"

DO 10 I = 1, N

C "Scaling the variables of integration"

```
call random(a)
call random(b)
call random(qaaa)
call random(qpaa)
call random(oqqpa)
call random(oqpa)
call random(phia)
call random(oqka)
call random(oqpka)
```

```
p= aa*a+0
```

```
q= vq*qaaa+2*10**6
qp= vqp*qpaa+2*10**6
qo= q
qop= qp
```

```
u= ab*b-1
oqqp= voloqqp*oqqpa+0
oqp= voloqp*oqpa+0
phi= volphi*phia+0
oqk= voloqk*oqka+0
oqpk= voloqpk*oqpka+0
```

C "Defining Variables within the loop"

```
e= SQRT((p)**2 + (m)**2)
ka= qo**2+qop**2+e**2+2*qo*(qop-e)-2*e*qop-(qp+q-p)**2-(m)**2
kb= 2*(qo+qop-e-(q+qp-p))
k= ka/kb
pp= p+k-q-qp
ep= SQRT((p + k - q - qp)**2 + (m)**2)
w= ep + qo + qop - e
```

```
if (e.lt.0) then
equation=0
go to 50
endif
```

```
if (k.lt.0) then
equation=0
```

```
go to 50
endif
```

```
if (pp.lt.0) then
equation=0
go to 50
endif
```

```
if (ep.lt.0) then
equation=0
go to 50
endif
```

```
if (w.lt.0) then
equation=0
go to 50
endif
```

C "Defining the Fermi Distributions"

```
fe= 1.d0/(exp((e-mu)/kt)+1)
fep= 1.d0/(exp((ep-mu)/kt)+1)
fg= 1.d0/(exp(w/kt)-1)
```

C "Variables in the Amplitude"

```
qa= p+k
qae= e+w
qb= pp-k
qbe= ep-w
```

CC

C SECTION 5.1 - "Plasma frequency Calculations"

```
nn=10000
```

```
lambda= kt/m
v= mu/kt
```

```
vola= 0.6-1.d0/(lambda)
volb= 32-1.d0/(lambda)
volc= 0.6-1.d0/(lambda)
vold= 27-1.d0/(lambda)
```

```
suma= 0
sumb= 0
sumc= 0
sumd= 0
```

C "Start of sub-do-loop"

```
DO 100 ii = 1, nn

call random(xxa)

xa=vola*xxa+(1.d0/lambda)

suma=suma+(lambda)**2*(xa**2-(1.d0)/lambda**2)/(exp(xa+v)+1)

call random(xxb)

xb=volb*xxb+(1.d0/lambda)

sumb=sumb+(lambda)**2*(xb**2-(1.d0)/lambda**2)/(exp(xb-v)+1)

call random(xxc)

xc=volc*xxc+(1.d0/lambda)

sumc=sumc+(1.d0/xc**2)*(xc**2-(1.d0)/lambda**2)/(exp(xc+v)+1)

call random(xxd)

xd=vold*xxd+(1.d0/lambda)

sumd=sumd+(1.d0/xd**2)*(xd**2-(1.d0)/lambda**2)/(exp(xd-v)+1)
```

100 continue

C "End of sub-do-loop"

```
ga= vola*suma/dble(nn)
gb= volb*sumb/dble(nn)
gc= volc*sumc/dble(nn)
gd= vold*sumd/dble(nn)
```

```
g= 2*ga+2*gb+gc+gd
woa= ((4*alpha*m**2)*g)/(9.42478*hbar**2)
wo= woa*hbar**2
```

C "Variables in the amplitude that require wo"

```
ba= 2*(-w*e+k*p)+wo
bb= -2*(-w*ep+k*pp)+wo
```

C END OF SECTION 5.1

CC

C SECTION 5.2 - "Dot products in the Amplitude"

```
ha= u
hb= cos(oqp)
hc= cos(oqpp)
hd= cos(oqp)*cos(oqpp)+sin(oqp)*sin(oqpp)*cos(phi)
```

```
kq= k*q*cos(oqk)
kqp= k*qp*cos(oqpk)
kpp= k*p*ha+k*k-kq-kqp
ppq= p*q*hb+kq-q*q-qp*q*hc
ppqp= p*qp*hd+kqp-q*qp*hc-qp*qp
pppp= p*p+k*p*ha-q*p*hb-qp*p*hd
```

C Dot Product between g[a,b] & g[a,b]
gg= 4

- C Dot Product between p & q
pqa= (e*qo-p*q*hb)
- C Dot Product between p & qp
pqb= (e*qop-p*qp*hd)
- C Dot Product between pp & q
ppqa= (ep*qo-ppq)
- C Dot Product between pp & qp
ppqb= (ep*qop-ppqp)
- C Dot Product between p & pp
ppp= (ep*e-pppp)
- C Dot Product between p & qa
qap= (e*e+w*e-p*p-k*p*ha)
- C Dot Product between pp & qa
qapp= (e*ep+w*ep-pppp-kpp)
- C Dot Product between p & qb
qbp= (ep*e-w*e-pppp+k*p*ha)
- C Dot Product between pp & qb
qbpp= (ep*ep-w*ep-pp*pp+kpp)
- C Dot Product between q & qp
qqp= (qo*qop-q*qp*hc)
- C Dot Product between q & qa
qaqa= (e*qo+k*qo-p*q*hb-kq)
- C Dot Product between qp & qa
qaqb= (e*qop+k*qop-p*qp*hd-kqp)
- C Dot Product between qa & qa
qaeqa= (e*e+w*w+2*e*w-p*p-k*k-2*p*k*ha)
- C Dot Product between q & qb
qbqa= (ep*qo-w*qo-ppq+kq)
- C Dot Product between qp & qb
qbqb= (ep*qop-w*qop-ppqp+kqp)
- C Dot Product between qb & qb
qbeqb= (ep*ep+w*w-2*ep*w-pp*pp-k*k+2*kpp)
- C Dot Product between qa & qb
qqq= (e*ep-e*w+w*ep-w*w-pppp+p*k*ha-kpp+k*k)
- C Dot Product between (e&qa) & (e&qp)
eqaeqp= -qaqb

- C Dot Product between (e&qa) & (e&q)
eqaeq= -qaqa
- C Dot Product between (e&pp) & (e&qp)
eppeqp= -ppqb
- C Dot Product between (e&pp) & (e&q)
eppeq= -ppqa

- C Dot Product between (e&q) & (e&qb)
eqeqb= -qbqa
- C Dot Product between (e&q) & (e&qp)
eqeqp= -qpp
- C Dot Product between (e&pp) & (e&qb)
eppeqb= -qbpp

- C Dot Product between (e&qa) & (e&qb)
eqaeqb= -qqq
- C Dot Product between (e&pp) & (e&qa)
eppeqa= -qapp
- C Dot Product between (e&qa) & (e&qa)
eqaeqa= -qaeqa

- C Dot Product between (e&qb) & (e&q)
eqbeq= -qbqa
- C Dot Product between (e&qb) & (e&qp)
eqbeqp= -qbqb
- C Dot Product between (e&pp) & (e&p)
eppep= -ppp

- C Dot Product between (e&p) & (e&qb)
epeqb= -qbp
- C Dot Product between (e&p) & (e&qa)
epeqa= -qap

C END OF SECTION 5.2

CC

C SECTION 5.3 - "First Part of the Amplitude: (Cv**2+Ca**2), mma"

$$s = (cv^{**2} + ca^{**2})$$

$taa = -4 * qaeqa * ppqa * pqb + 4 * qaeqa * qqp * ppp - 4 * qaeqa * pqa * ppqb$
 $tab = 8 * qap * ppqb * qaqa + 8 * qap * ppqa * qaqb - 8 * qqp * qap * qapp$
 $tac = -4 * qaeqa * ppp + 4 * qaeqa * gg * ppp - 4 * qaeqa * ppp + 8 * qap * qapp$
 $tad = 8 * qap * qapp - 8 * gg * qap * qapp$
 $tae = -4 * qaeqa * ppqb * pqa + 4 * qaeqa * qqp * ppp - 4 * qaeqa * pqb * ppqa$
 $taf = 8 * qap * ppqa * qaqb + 8 * qap * ppqb * qaqa - 8 * qap * qapp * qqp$

$ta = taa + tab - qqp * (tac + tad) + tae + taf$

$tba = -4 * ppqb * qaqa + 4 * qqp * qapp - 4 * ppqa * qaqb$
 $tbb = -4 * qapp + 4 * gg * qapp - 4 * qapp$
 $tbc = -4 * ppqa * qaqb + 4 * qapp * qqp - 4 * ppqb * qaqa$

$tb = tba - qqp * (tbb) + tbc$

$tca = 4 * pqb * ppqa - 4 * qqp * ppp + 4 * pqa * ppqb$
 $tcb = 4 * ppp - 4 * gg * ppp + 4 * ppp$
 $tcc = 4 * pqa * ppqb - 4 * qqp * ppp + 4 * pqb * ppqa$

$tc = tca - qqp * (tcb) + tcc$

$tda = -4 * ppqb * qaqa + 4 * qqp * qapp - 4 * ppqa * qaqb$
 $tdb = -4 * qapp + 4 * gg * qapp - 4 * qapp$
 $tdc = -4 * ppqa * qaqb + 4 * qqp * qapp - 4 * ppqb * qaqa$

$td = tda - qqp * (tdb) + tdc$

$tea = -4 * pqb * qapp * qbqa - 4 * qap * ppqb * qbqa + 8 * eqaeqp * ppp * qbqa$
 $teb = 4 * ppp * qaqb * qbqa - 8 * eppeqp * qap * qbqa + 4 * pqb * qbpp * qaqa$
 $tec = -4 * qbp * ppqb * qaqa + 4 * pqb * ppqa * qqg + 4 * pqa * ppqb * qqg$
 $ted = -4 * pqb * ppqa * qaqb - 4 * pqa * qbpp * qaqb + 8 * eqeqb * ppp * qaqb$
 $tee = -8 * eqeqb * qap * ppqb + 8 * eqeqp * pqb * qapp + 4 * qqp * qbp * ppqa$
 $tef = -8 * eqaeqp * pqb * qapp + 4 * ppp * qaqa * qbqb + 4 * qap * ppqa * qbqb$
 $teg = -4 * pqa * qapp * qbqb + 8 * eppeqb * qbp * qaqa - 8 * eppeqp * qbp * qaqa$
 $teh = 8 * eqaeqb * pqb * ppqa - 8 * eqaeqp * qbp * ppqa + 8 * eqaeqb * pqa * ppqb$
 $tei = -8 * eqaeqp * pqa * qbpp + 8 * eqeqp * qap * qbpp + 4 * qqp * qap * qbpp$
 $tej = -8 * eqaeqb * qqp * ppp - 8 * eppeqb * pqa * qaqb + 8 * eppeqp * pqa * qqg$
 $tek = -8 * eqeqp * ppp * qqg - 4 * qqp * ppp * qqg + 8 * eppeqb * qqp * qap$
 $tel = -4 * qapp * qbp - 4 * qap * qbpp + 8 * ppp * eqaeqb$
 $tem = 4 * ppp * qqg - 8 * qap * eppeqb + 4 * qbpp * qap$
 $ten = -4 * qbp * qapp + 4 * qqg * ppp + 4 * qqg * ppp$

teo=-4*qb* qapp-4*qbpp* qap+8*ppp* eqaeqb
 tep=-8* qap* eppeqb-8* qappqb+4* qb* ppqa* gg
 teq=-8* qapp* epeqb+4* ppp* qq+4* qap* qbpp
 ter=-4* qapp* qb+8* eppeqb* qap-8* qb* eppeqa
 tes=8* eqaeqb* ppp-8* qb* eppeqa+8* eqaeqb* ppp
 tet=-8* qbpp* epeqa-8* qap* qbpp+4* qap* qbpp* gg
 teu=-8* eqaeqb* ppp* gg-8* eppeqb* qap+8* qq* eppep
 tev=8* ppp* qq-4* gg* ppp* qq+8* eppeqb* gg* qap
 tew=-4* qapp* pqa* qbqb-4* qap* ppqa* qbqb+8* ppp* eqaeq* qbqb
 tex=4* ppp* qaqa* qbqb-8* qap* eppeq* qbqb+4* qbpp* qaqa* pqa
 tey=-4* qb* qaqa* ppqa+4* qq* ppqb* pqa+4* qq* ppqa* pqb
 tez=-4* qb* qaqa* ppqb-4* qbpp* pqb* qaqa+8* ppp* eqbeqp* qaqa
 teza=-8* qap* eqbeqp* ppqa+8* qapp* pqb* eqeqp+4* qq* qb* ppqa
 tezb=-8* qapp* pqa* eqbeqp+4* ppp* qaqa* qbqa+4* qap* ppqb* qbqa
 tezc=-4* qapp* pqb* qbqa+8* eppeqb* pqa* qaqa-8* qb* qaqa* eppeq
 tezd=8* eqaeqb* ppqb* pqa-8* qb* eqaeq* ppqb+8* eqaeqb* pqb* ppqa
 teze=-8* qbpp* eqaeq* pqb+8* eqeqp* qap* qbpp+4* qq* qap* qbpp
 tez=-8* eqaeqb* qq* ppp-8* eppeqb* pqb* qaqa+8* qq* pqb* eppeq
 tezg=-8* eqeqp* ppp* qq-4* qq* ppp* qq+8* eppeqb* qq* qap

teaa=tea+teb+tec+ted+tee+tef+teg+teh+tei+tej+tek
 tebb=tel+tem+ten+teo+tep+teq+ter+tes+tet+teu+tev
 tecc=tew+tex+tey+tez+teza+tezb+tezc+tezd+teze+tezf+tezg

te=teaa - qq*(tebb) + tecc

tfa=-4* qapp* qbqa* pqb+4* qap* qbqa* ppqb+4* ppp* qbqa* qaqa
 tfb=-4* qbpp* qaqa* pqb-4* qb* qaqa* ppqb+8* ppp* qaqa* eqbeqp
 tfc=4* qq* ppqa* pqb+4* qq* pqa* ppqb-4* qb* ppqa* qaqa
 tfd=4* qbpp* qaqa* pqa+8* eqaeqb* pqb* ppqa-8* qap* eqbeqp
 tfe=8* eqaeqb* ppqb* pqa-8* qapp* pqa* eqbeqp+8* qapp* qb* eqeqp
 tff=4* qb* qapp* qq-8* ppp* eqaeqb* qq+4* ppp* qaqa* qbqb
 tfg=-4* qap* ppqa* qbqb-4* qapp* qbqb* pqa+8* qbqa* ppp* eqaeq
 tfh=-8* qap* qbqb* eppeq-8* eppeqb* qaqa* pqb-8* qb* ppqb* eqaeq
 tfi=8* qap* qbpp* eqeqp+4* qap* qbpp* qq-8* qbpp* pqb* eqaeq
 tfj=8* eppeqb* pqa* qaqa-8* qb* qaqa* eppeq-8* ppp* qq* eqeqp
 tfk=-4* ppp* qq* qq+8* qq* pqb* eppeq+8* qap* eppeqb* qq

tfl=-4* qapp* qb+4* qap* qbpp+4* ppp* qq
 tfm=-4* qbpp* qap-4* qb* qapp+8* ppp* eqaeqb
 tfn=4* qq* ppp+4* qq* ppp-4* qb* qapp
 tfo=4* qbpp* qap+8* eqaeqb* ppp-8* qap* eppeqb
 tfp=8* eqaeqb* ppp-8* qapp* epeqb-8* qapp* qb
 tfq=4* qb* qapp* gg-8* ppp* eqaeqb* gg+4* ppp* qq

$tfr = -4 * qap * qbpp - 4 * qapp * qbp + 8 * ppp * eqaeqb$
 $tfs = -8 * qap * eppeqb - 8 * eppeq * qap - 8 * qbp * eppeqa$
 $tft = -8 * qap * qbpp + 4 * qap * qbpp * gg - 8 * qbpp * eppeqa$
 $tfu = 8 * eppeq * qap - 8 * qbp * eppeqa + 8 * ppp * qq$
 $tfv = -4 * ppp * qq * gg + 8 * qq * eppep + 8 * qap * eppeqb * gg$

$tfw = -4 * qapp * qbqb * pqa + 4 * qap * qbqb * ppqa + 4 * ppp * qbqb * qaqa$
 $tfx = -4 * qbpp * qaqb * pqa - 4 * qbp * qaqb * ppqa + 8 * ppp * qaqb * eqeqb$
 $tfy = 4 * qq * ppqb * pqa + 4 * qq * pqb * ppqa - 4 * qbp * ppqb * qaqa$
 $tfz = 4 * qbpp * qaqa * pqb + 8 * eqaeqb * pqa * ppqb - 8 * qap * eqeqb$
 $tfza = 8 * eqaeqb * ppqa * pqb - 8 * qapp * pqb * eqeqb + 8 * qapp * qbp * eqeqp$
 $tfzb = 4 * qbp * qapp * qqr - 8 * ppp * eqaeqb * qqr + 4 * ppp * qaqb * qbqa$
 $tfzc = -4 * qap * ppqb * qbqa - 4 * qapp * qbqa * pqb + 8 * ppp * qbqb * eqaeq$
 $tfzd = -8 * qap * qbqb * eppeqp - 8 * eppeq * qaqb * pqa - 8 * qbp * ppqa * eqaeqp$
 $tfze = 8 * qap * qbpp * eqeqp + 4 * qap * qbpp * qqr - 8 * qbpp * pqa * eqaeqp$
 $tfzf = 8 * eppeq * pqb * qaqa - 8 * qbp * qaqb * eppeqp - 8 * ppp * qq * eqeqp$
 $tfzg = -4 * ppp * qq * qqr + 8 * qq * pqa * eppeqp + 8 * qap * eppeqb * qqr$

$tfaa = tfa + tfb + tfc + tfd + tfe + tff + tfg + tfh + tfi + tfj + tfk$
 $tfbb = tfl + tfm + tfn + tfo + tfp + tfq + tfr + tfs + tft + tfu + tfv$
 $tfcc = tfw + tfx + tfy + tfz + tfza + tfzb + tfzc + tfzd + tfze + tfzf + tfzg$

$tf = tfaa - qqp * (tfbb) + tfcc$

$tga = -4 * ppqb * qbqa + 8 * eqbeqp * ppqa - 8 * eqeqp * qbpp - 4 * qqr * qbpp$
 $tgb = 4 * ppqa * qbqb + 8 * eppeq * qbqb - 8 * eppeq * qqr$
 $tgc = -4 * qbpp + 8 * eppeq + 8 * qbpp - 4 * gg * qbpp + 4 * qbpp$
 $tgd = 8 * eppeq - 8 * gg * eppeq$
 $tge = -4 * ppqa * qqbb + 8 * ppqb * eqbeq - 8 * eqeqp * qbpp - 4 * qqr * qbpp$
 $tgf = 4 * ppqb * qbqa + 8 * qbqa * eppeqp - 8 * eppeq * qqr$

$tg = tga + tgb - qqp * (tgc + tgd) + tge + tgf$

$tha = 8 * eppeqp * qbqa + 4 * ppqb * qbqa - 8 * eqeqp * qbpp - 4 * qqr * qbpp$
 $thb = 8 * eqaeq * ppqb - 4 * ppqa * qbqb - 8 * eppeq * qqr$
 $thc = 8 * eppeq + 4 * qbpp + 8 * qbpp - 4 * gg * qbpp + 8 * eppeq$
 $thd = -4 * qbpp - 8 * gg * eppeq$
 $the = 8 * qbqb * eppeq + 4 * ppqa * qbqb - 8 * eqeqp * qbpp - 4 * qqr * qbpp$
 $thf = 8 * ppqa * eqbeqp - 4 * ppqb * qbqa - 8 * eppeq * qqr$

$th = tha + thb - qqp * (thc + thd) + the + thf$

$tia=4*pcb*qaqa-8*eqeap*gap-4*qqp*gap+8*eqaeq*pcb-4*pqa*qaqb$
 $tib=4*gap+8*gap-4*gg*gap+8*eqaeq-4*gap$
 $tic=4*pqa*qaqb-8*eqeap*gap-4*qqp*gap+8*pqa*eqaeq-4*pcb*qaqa$

$ti=tia - qqp*(tib) + tic$

$tja=-4*pcb*qaqa+8*eqaeq*pqa-8*eqeap*gap-4*qqp*gap+4*pqa*qaqb$
 $tjb=-4*gap+8*eqaeq+8*gap-4*gg*gap+4*gap$
 $tjc=-4*pqa*qaqb+8*pcb*eqaeq-8*eqeap*gap-4*qqp*gap+4*pcb*qaqa$

$tj=tja - qqp*(tjb) + tjc$

$tka=16*eqeap+8*qqp$
 $tkb=-16+8*gg$
 $tkc=16*eqeap+8*qqp$

$tk=tka - qqp*(tkb) + tkc$

$tla=4*pcb*qbpp*qbqa+4*qb*ppqb*qbqa-4*ppp*qbqb*qbqa$
 $tlb=8*eppeqb*pcb*qbqa+8*eppeq*qb*qbqa+4*pcb*qbpp*qbqa$
 $tlc=-4*qb*ppqb*qbqa-4*pcb*ppqa*qbqb-4*pqa*ppqb*qbqb$
 $tl d=4*qb*ppqa*qbqb+4*pqa*qbpp*qbqb-4*qqp*qb*qbpp$
 $tle=4*ppp*qbqa*qbqb-4*qb*ppqa*qbqb+4*pqa*qbpp*qbqb$
 $tlf=8*eppeqb*pqa*qbqb-8*eppeq*qb*qbqb+8*eppeqb*pcb*qbqa$
 $tlg=-8*eppeq*qb*qbqa-4*qqp*qb*qbpp+8*eppeqb*pqa*qbqb$
 $tlh=8*eppeq*qb*qbqb-8*eppeq*pqa*qbqb+4*qqp*ppp*qbqb$
 $tli=-8*eppeq*pcb*qbqb-8*eppeqb*qqp*qb-8*eppeqb*qqp*qb$
 $tlj=4*qbpp*qb+4*qb*qbpp-4*ppp*qbqb$
 $tlk=8*eppeqb*qb+8*qb*eppeqb+4*qbpp*qb$
 $tl l=-4*qb*qbpp-4*qbqb*ppp-4*qbqb*ppp$
 $tlm=4*qb*qbpp+4*qbpp*qb-4*qb*qbpp*gg$
 $tl n=4*ppp*qbqb-4*qb*qbpp+4*qbpp*qb$
 $tl o=8*eppeqb*qb-8*qb*eppeqb+8*eppeqb*qb$
 $tlp=-8*qb*eppeqb-4*qb*qbpp*gg+8*eppeqb*qb$
 $tlq=8*qb*eppeqb-8*qbqb*eppep+4*ppp*qbqb*gg$
 $tlr=-8*qbqb*eppep-8*eppeqb*qb*gg-8*eppeqb*qb*gg$
 $tl s=4*qbpp*pqa*qbqb+4*qb*ppqa*qbqb-4*ppp*qbqa*qbqb$
 $tl t=8*eppeqb*pqa*qbqb+8*qb*qbqb*eppeq+4*qbpp*qbqb*pqa$
 $tl u=-4*qb*qbqb*ppqa-4*qbqb*ppqb*pqa-4*qbqb*pcb*ppqa$
 $tl v=4*qb*ppqb*qbqa+4*qbpp*pcb*qbqa-4*qqp*qb*qbpp$
 $tl w=4*ppp*qbqb*qbqa-4*qb*ppqb*qbqa+4*qbpp*pcb*qbqa$
 $tl x=8*eppeqb*pcb*qbqa-8*qb*eppeq*qbqa+8*eppeqb*qbqb*pqa$

$tly = -8 * qbp * eppeq * qbqb - 4 * qbp * qbpp * qqp + 8 * eppeq * pqb * qbqa$
 $tlz = 8 * qbp * qbqa * eppeq - 8 * qbeqb * eppeq * pqb + 4 * qqp * ppp * qbeqb$
 $tlza = -8 * qbeqb * eppeq * pqb - 8 * eppeq * qbp * qqp - 8 * eppeq * qqp * qbp$

$tlaa = tla + tlb + tlc + tld + tle + tlf + tlg + tlh + tli$
 $tlbb = tlj + tlk + tll + tlm + tln + tlo + tlp + tlq + tlr$
 $tlcc = tls + tlt + tlu + tlw + tlx + tly + tlz + tlza$

$tl = tlaa - qqp * (tlbb) + tlcc$

$tma = 4 * pqb * ppqa + 8 * eppeq * pqa - 4 * qqp * ppp + 8 * eppeq * pqb + 4 * pqa * ppqb$
 $tmb = 4 * ppp + 8 * eppeq - 4 * gg * ppp + 8 * eppeq + 4 * ppp$
 $tmc = 4 * pqa * ppqb + 8 * pqb * eppeq - 4 * qqp * ppp + 8 * pqa * eppeq + 4 * pqb * ppqa$

$tm = tma - qqp * (tmb) + tmc$

$tna = -4 * pqb * qbqa + 4 * qqp * qbp - 4 * pqa * qbqb$
 $tnb = -4 * qbp + 4 * gg * qbp - 4 * qbp$
 $tnc = -4 * pqa * qbqb + 4 * qqp * qbp - 4 * pqb * qbqa$

$tn = tna - qqp * (tnb) + tnc$

$toa = -4 * pqb * qbqa + 4 * qqp * qbp - 4 * pqa * qbqb$
 $tob = -4 * qbp + 4 * gg * qbp - 4 * qbp$
 $toc = -4 * pqa * qbqb + 4 * qqp * qbp - 4 * pqb * qbqa$

$to = toa - qqp * (tob) + toc$

C "Defining the First Part of the Amplitude: mma"

$mmaa = s * (1.d0/ba**2) * (ta + (m**2) * (tb + tc + td))$
 $mmab = s * (1.d0/(ba*bb)) * (te + tf + (m**2) * (tg + th + ti + tj)) + (m**4) * (tk)$
 $mmac = s * (1.d0/bb**2) * (tl + (m**2) * (tm + tn + to))$

$mma = mmaa + mmab + mmac$

C END OF SECTION 5.3

CC

CC

C SECTION 5.4 - "Second Part of the Amplitude: (Cv**2-Ca**2), mmb"

$$ss = (cv**2 - ca**2)$$

$$\begin{aligned} raa &= 4 * pqb * qaqa + 4 * qqp * qap - 4 * pqa * qaqb \\ rab &= 4 * qap + 4 * gg * qap - 4 * qap \\ rac &= 4 * pqa * qaqb + 4 * qqp * qap - 4 * pqb * qaqa \end{aligned}$$

$$ra = raa - qqp * (rab) + rac$$

$$\begin{aligned} rba &= -4 * qaeqa * qqp \\ rbb &= -4 * gg * qaeqa \\ rbc &= -4 * qaeqa * qqp \end{aligned}$$

$$rb = rba - qqp * (rbb) + rbc$$

$$\begin{aligned} rca &= -4 * pqb * qaqa + 4 * qqp * qap + 4 * pqa * qaqb \\ rcb &= -4 * qap + 4 * gg * qap + 4 * qap \\ rcc &= -4 * pqa * qaqb + 4 * qqp * qap + 4 * pqb * qaqa \end{aligned}$$

$$rc = rca - qqp * (rcb) + rcc$$

$$\begin{aligned} rda &= -4 * qqp \\ rdb &= -4 * gg \\ rdc &= -4 * qqp \end{aligned}$$

$$rd = rda - qqp * (rdb) + rdc$$

$$\begin{aligned} rea &= 8 * eppeqp * qaqa + 4 * ppqb * qaqa + 8 * eqaeqp * ppqa - 8 * eqeqp * qapp \\ reb &= -4 * qqp * qapp + 4 * ppqa * qaqb \\ rec &= 8 * eppeqa + 4 * qapp + 8 * eppeqa + 8 * qapp \\ red &= -4 * gg * qapp + 4 * qapp \\ ree &= 8 * qaqb * eppeq + 4 * ppqa * qaqb + 8 * ppqb * eqaeq - 8 * eqeqp * qapp \\ ref &= -4 * qqp * qapp + 4 * ppqb * qaqa \end{aligned}$$

$$re = rea + reb - qqp * (rec + red) + ree + ref$$

$rfa = -4 * pqb * ppqa - 8 * eppeq * pqa + 8 * eqeqp * ppp + 4 * qqp * ppp - 4 * pqa * ppqb$
 $rfb = -4 * ppp - 8 * eppeq - 8 * ppp + 4 * gg * ppp - 4 * ppp$
 $rfc = -4 * pqa * ppqb - 8 * eppeq * pqb + 8 * eqeqp * ppp + 4 * qqp * ppp - 4 * pqb * ppqa$

$rf = rfa - qqp * (rfb) + rfc$

$rga = -4 * pqb * ppqa + 8 * eqeqp * ppp + 4 * qqp * ppp - 8 * eppeq * pqb - 4 * pqa * ppqb$
 $rgb = -4 * ppp - 8 * ppp + 4 * gg * ppp - 8 * eppeq - 4 * ppp$
 $rgc = -4 * pqa * ppqb + 8 * eqeqp * ppp + 4 * qqp * ppp - 8 * pqa * eppeq - 4 * pqb * ppqa$

$rg = rga - qqp * (rgb) + rgc$

$rha = 4 * ppqb * qaqa - 8 * eqeqp * qapp - 4 * qqp * qapp + 8 * eqaeq * ppqb + 4 * ppqa * qaqb$
 $rhb = 8 * eppeq * qaqb$
 $rhc = 4 * qapp + 8 * qapp - 4 * gg * qapp + 8 * eppeqa + 4 * qapp$
 $rhd = 8 * eppeqa$
 $rhe = 4 * ppqa * qaqb - 8 * eqeqp * qapp - 4 * qqp * qapp + 8 * ppqa * eqaeq + 4 * ppqb * qaqa$
 $rhf = 8 * eppeq * qaqa$

$rh = rha + rhb - qqp * (rhc + rhd) + rhe + rhf$

$ria = -8 * eqaeq * qbqa - 4 * qaqb * qbqa + 8 * eqeqp * qq + 4 * qqp * qq$
 $rib = -8 * eqbeq * qaqb - 4 * qaqa * qbqb + 8 * eqaeq * qq$
 $ric = -8 * eqaeq - 4 * qq + 8 * eqaeq + 4 * gg * qq$
 $rid = -8 * eqaeq - 4 * qq + 8 * gg * eqaeq$
 $rie = -8 * qbqb * eqaeq - 4 * qaqa * qbqb + 8 * eqeqp * qq + 4 * qqp * qq$
 $rif = -8 * qaqa * eqbeq - 4 * qaqb * qbqa + 8 * eqaeq * qq$

$ri = ria + rib - qqp * (ric + rid) + rie + rif$

$rja = 4 * pqb * qbqa - 8 * eqeqp * qbp - 4 * qqp * qbp + 8 * eqbeq * pqb + 4 * pqa * qbqb$
 $rjb = 4 * qbp + 8 * qbp - 4 * gg * qbp + 8 * epqb + 4 * qbp$
 $rjc = 4 * pqa * qbqb - 8 * eqeqp * qbp - 4 * qqp * qbp + 8 * pqa * eqbeq + 4 * pqb * qbqa$

$rj = rja - qqp * (rjb) + rjc$

$rka = 4 * pqb * qbqa + 8 * eqbeq * pqa - 8 * eqeqp * qbp - 4 * qqp * qbp + 4 * pqa * qbqb$
 $rkb = 4 * qbp + 8 * epqb + 8 * qbp - 4 * gg * qbp + 4 * qbp$

$$rkc=4*pqa*qbqb+8*pqb*eqeqb-8*eqeqp*qbp-4*qqp*qbp+4*pqb*qbqa$$

$$rk=rka - qqp*(rkb) + rkc$$

$$rla=-4*qaqb*qbqa-8*eqbeqp*qaqa+8*eqeqp*qqq+4*qqp*qqq$$

$$rlb=8*eqaeqb*qqp-4*qaqa*qbqb-8*eqaeq*qbqb$$

$$rlc=-4*qqq-8*eqaeqb-8*qqq+4*gg*qqq$$

$$rld=8*gg*eqaeqb-4*qqq-8*eqaeqb$$

$$rle=-4*qaqa*qbqb-8*qaqb*eqeqb+8*eqeqp*qqq+4*qqp*qqq$$

$$rlf=8*eqaeqb*qqp-4*qaqb*qbqa-8*eqaeqp*qbqb$$

$$rl=rla+rlb - qqp*(rlc+rld) + rle+rlf$$

$$rma=8*eppeqp*qbqa+4*ppqb*qbqa+4*qqp*qbpp-4*ppqa*qbqb$$

$$rmb=-8*eppeq*qbqb+8*eppeqb*qqp$$

$$rnc=-8*eppeqb-4*qbpp+4*gg*qbpp+4*qbpp$$

$$rmd=8*eppeqb+8*gg*eppeqb$$

$$rme=8*eppeq*qbqb+4*ppqa*qbqb+4*qqp*qbpp-4*ppqb*qbqa$$

$$rmf=-8*eppeqp*qbqa+8*qqp*eppeqb$$

$$rm=rma+rmb - qqp*(rnc+rmd) + rme+rmf$$

$$rna=-8*eppeqp*qbqa-4*ppqb*qbqa+4*qqp*qbpp+4*ppqa*qbqb$$

$$rnb=8*eppeq*qbqb+8*eppeqb*qqp$$

$$rnc=-8*eppeqb-4*qbpp+4*gg*qbpp+4*qbpp$$

$$rnd=8*eppeqb+8*gg*eppeqb$$

$$rne=-8*eppeq*qbqb-4*ppqa*qbqb+4*qqp*qbpp+4*ppqb*qbqa$$

$$rmf=8*eppeqp*qbqa+8*eppeqb*qqp$$

$$rn=rna+rnb - qqp*(rnc+rnd) + rne+rmf$$

$$roa=-4*qbeqb*qqp$$

$$rob=-4*qbeqb*gg$$

$$roc=-4*qbeqb*qqp$$

$$ro=roa - qqp*(rob) + roc$$

$$rpa=-4*qqp$$

$$rpb=-4*gg$$

$$rpc=-4*qqp$$

$$rp = rpa - qqp*(rpb) + rpc$$

C "Defining the Second Part of the Amplitude: mmb"

$$\begin{aligned} mmba &= ss*(1.d0/ba**2)*(m**2*(ra+rb+rc)+m**4*(rd)) \\ mmbb &= ss*(1.d0/(ba*bb))*(m**2*(re+rf+rg+rh+ri+rj+rk+rl)) \\ mmbc &= ss*(1.d0/bb**2)*(m**2*(rm+rn+ro)+m**4*(rp)) \\ mmb &= mmba+mmbb+mmbc \end{aligned}$$

C END OF SECTION 5.4

CC

C SECTION 5.5 - "The Final Form of the Amplitude: mm"

$$\begin{aligned} mm &= constb*(mma+mmb) \\ \text{if (mm.lt.0) then} \\ \text{equation} &= 0 \\ \text{go to 50} \\ \text{endif} \end{aligned}$$

C END OF SECTION 5.5

CC

C SECTION 5.6 - "Addition of the Function and function Squared"

C "Units are eV*cm**2"

$$\begin{aligned} y &= consta*p**2*fe*k**2*fg*(1-fep)*(e+w-ep)*mm \\ z &= (e*w*ep*qo*qop) \\ \text{equation} &= y/z \end{aligned}$$

50 continue

C "Changes units to 1/ergs**5/cc/s"

C "In order to calculate emissivity instead of rate"

C "One must remove ergs from equation below!!!"

two= 1.d0/(10**6)
ergs= 1.602*two**2
con= 1/((hbar)**6*c**5)

units= con*ergs

f= f + (units*equation)
fsquared= fsquared + (units*equation)**2

C END OF SECTION 5.6

CC

10 continue

C END OF SECTION 5 - "End of Do Loop"

CC

C SECTION 6 - "Calculating the dQphoto and its Uncertainty"

dQphoto= vol*f/dble(N)
uncertainty= vol*SQRT((fsquared/dble(N)-(f/dble(N))**2)/dble(N))

C END OF SECTION 6

CC

CC

C SECTION 6.1 - "Addition of the Function and function Squared"

```
ff= ff + (8*3.14159**2*dQphoto*q**2*qp**2*sin(oqqp))
ffsq= ffsq + (8*3.14159**2*dQphoto*q**2*qp**2*sin(oqqp))**2
```

C END OF SECTION 6.1

CC

1000 continue

C END OF SECTION 6 - "End of Do Loop"

CC

C SECTION 7 - "Calculating the Qphoto and its Uncertainty"

```
Qphoto= ff*volqphoto/dble(nnn)
uncerta= SQRT((ffsq/dble(nnn)-(ff/dble(nnn))**2)/dble(nnn))
uncert= volqphoto*uncerta
```

C END OF SECTION 7

CC

C SECTION 8 - "Displaying Results"

```
print *, 'Qphoto'
print *, Qphoto
print *, 'Uncertainty'
```

```
print *, uncert
print *, 'dQphoto'
print *, dQphoto
print *, 'Uncertainty'
print *, uncertainty
print *, 'plasma stuff'
print *, g
print *, woa
print *, wo
print *, ba
print *, 'Functions'
print *, fe
print *, fep
print *, fg
print *, 'Energy'
print *, e
print *, ep
print *, w
print *, k
print *, pp
print *, 'Amplitude'
print *, mm
print *, mma
print *, mmb
print *, 'Random Variables'
print *, p
print *, u
```

C "END OF PROGRAM Photo Neutrino Emissivity

end

C END OF SECTION 8

CC

C SECTION 9 - "Random Number Generator 0 -> 1"

SUBROUTINE random (rannum)

```
integer n, const1
real rannum, const2
parameter (const1 = 2147483647, const2 = .4656613E-9)
save
data n /0/

if (n .eq. 0) n = int(rannum)
n = n * 65539
if (n .lt. 0) n = (n + 1) + const1
rannum = n * const2

end
```

C END OF SECTION 9

```
CCCCCCCCCCCCCCCCCCCCCCCCCCCCCCCCCCCCCCCCCCCCCCCCCCCCCCCCCCCC
CCCCCCCCCCCCCCCCCCCCCCCCCCCCCCCCCCCCCCCCCCCCCCCCCCCCCCCCCCCC
```

References

- Aglietta, M., et al. 1987, *Europhysics Lett.*, 3, 1315
- Bahcall, J. N. & Meszaros, P. 2000, *Phys. Rev.*, 85, 7
- Beudet, G., Petrosian, V., and Salpeter, E. E. 1967, *ApJ*, 150, 979
- Becker, P. A. et al. 2001, *ApJ*, 552, 209
- Burrows, A. & Lattimer, J. 1987, *ApJ*, 318, L63
- Davies, M. B., Benz, W., & Hills, J. G. 1991, *ApJ*, 381, 449
- Dicus, D. A. 1973, *Phys. Rev. D*, 6, 941
- Fargion, D. 2001, *astro-ph/0103276*
- Fryer, C. L. & Heger, A. 2000, *ApJ*, 541, 1033
- Fryer, C. L. & Woosley, S. E. 1998, *ApJ*, 502, L9
- Fryer, C. L., Woosley, S. E., Herant, M., & Davies, M. B. 1999, *ApJ*, 520, 650
- Fynbo, J. U. et al. 2000, *ApJ*, 542, L89
- Gammie, C. & Popham, R. 1998, *ApJ*, 504, 419
- Haft, M. et al. 1994, *ApJ*, 425, 222
- Haubold, H. J., et al. 1988, *A&A*, 191, 22
- Hillebrandt, W. et al. 1987, *A&A*, 180, L20
- Itoh, N. et al. 1990, *ApJ*, 339, 354
- Itoh, N. & Kohyama, Y. 1983, *ApJ*, 275, 858
- Janka, H.-Th., Eberl, T., Ruffert, M., & Fryer C. L. 1999, *ApJ*, 527, L39
- Janka, H.-Th. & Ruffert, M. 1996, *A&A*, 307, L33
- Kalos, M. H. & Whitlock, P. A. Monte Carlo Methods Volume I: Basics. A Wiley-Interscience Publications, 1986

- Kifonidis, K. et al. 2003, A&A, 408, 621
- Kohyama, Y. et al. 1993, ApJ, 415, 267
- Kolb, E. W. & Turner, M. S. 1990, The Early Universe: Frontiers in Physics. Addison-Wesley Publishing Company, 1990
- Lazzati, D. et al. 2001, A&A, 278, 996
- MacFadyen, A. I. & Woosley, S. E. 1999, ApJ, 524, 262
- Mahadevan, R. & Quataert, E. 1997, ApJ, 490, 605
- McLaughlin, G. C. et al. 2001, ApJ, 567, 454
- Meszaros, P. & Rees, J. 2000, ApJ, 541, L5
- Meszaros, P. & Waxman, E. 2001, Phys. Rev., 87, 17
- Munakata, H. et al. 1985, ApJ, 296, 197
- Nagataki, S. 2000, ApJS, 127, 141
- Narayan, R. et al. 1997, ApJ, 476, 49
- Prantzos, H., et al. 1988, 331, 15
- Raffelt, G. C. 2001, ApJ, 561, 890
- Saha, D. & Chattopadhyay, G. 1991, Ap&SS, 178, 209S
- Salam, A. 1968, in Proc. Eighth Nobel Symposium on Elementary Particle Theory, Relativistic Groups, and Analyticity, ed. N. Svartholm (Stockholm: Almqvist & Wiksells), p. 367
- Schinder, P. J. et al. 1987, ApJ, 313, 531
- Shakura, N. I. & Sunyaev, R. A. 1973, A&A, 24, 337
- Symbalisky, E. M. D. 1984, ApJ, 285, 729
- Tohline, J. E., et al. 1980, Space Sci. Rev., 27, 555
- Vishniac, E. T. & Wheeler, J. C. 1996, ApJ, 471, 921

Wang, Q. D. 1999, ApJ, 517, L27

Wang, L., et al. 2002, ApJ, 579, 671

Waxman, E. 2000, ApJ, 127, 2

Waxman, E. & Bahcall, J. 1997, Phys. Rev., 78, 12

Waxman, E. & Bahcall J. N. 2000, ApJ, 541, 707

Weinberg, S. 1967, Phys. Rev. Letters, 19, 1264

Woosley, S. E. 1993, ApJ, 405, 273

David MacInnis

92 Nita Dr.
Truro, Nova Scotia
B2N 6G7
(902) 893-3404 (Home)

EDUCATION:

2003-2007

Ph.D. in Physics, University of New Mexico, NM

2002-2003

M.Sc. in Physics, August 2003, University of New Mexico, NM

2000-2004

M.Sc. in Astronomy, Spring 2004, Saint Mary's University, Halifax, NS

1996-2000

B.Sc. in Physics and Mathematics, May 2000, McGill University, Montreal, PQ

1993-1996

High School Diploma, Honors with Distinction, Cobiquid Educational Centre, Truro, NS

RELEVANT EXPERIENCE:

2002-2004

TA for a first year astronomy lab. Duties included preparing lectures for classes as well as correcting assignments. Questions asked by students were answered with passion and vigor. Enthusiasm was demonstrated in the class to enhance the atmosphere.

2001-2002

Part-time faculty member at Saint Mary's University, teaching tutorials for a first-year physics course as well as their corresponding labs. Duties for the tutorials included preparing lectures and problems that was in parallel with the main lectures and helping students with their troubles. Duties for the labs involved preparing a short summary and demonstration of the lab at hand, along with helping the students throughout the lab. Corrections to formal labs was also performed.

2000-2001

First year physics lab assistant at Saint Mary's University. This involved helping the students during the lab as well as correcting the labs each week.

2000-2002

Marker and assistant for a first year physics course, Saint Mary's University.

2000-2002

Telescope tour guide for the public at the Burke-Gaffney Observatory, Saint Mary's University.